PHOTOCHEMICAL APPROACHES TO CONTROL CELL SURFACE RECEPTOR ACTIVATION WITH SPATIOTEMPORAL SPECIFICITY

A Dissertation

Presented to the Faculty of the Weill Cornell Graduate School

of Medical Sciences

in Partial Fulfillment of the Requirements for the Degree of

Doctor of Philosophy

by

Thinh Nguyen Duc.

February 2016

PHOTOCHEMICAL APPROACHES TO CONTROL CELL SURFACE RECEPTOR ACTIVATION WITH SPATIOTEMPORAL SPECIFICITY

Thinh Nguyen Duc, Ph.D.

Cornell University 2016

Over the last decade, there have been remarkable technological advances that have revitalized the age old idea that biology is first and foremost an observational science. Nowhere has this Galisonian ideal of scientific discovery been more realized than in the study of cell biology and signaling processes that govern a cell's functionalities. Imaging techniques, beginning with the advent of genetically encoded fluorescent proteins, to the more recent single molecule imaging techniques that allow for observation of biological processes at resolutions below the diffraction limit of light, have given scientists the ability to gaze deep into living cells and discern molecular processes. These technologies have more than ever illustrated that the cell is not merely an aqueous mixture of proteins and molecules enclosed in a lipid bilayer membrane, but rather a tightly organized structure where signaling processes can be highly anisotropic. Detailed observations of cellular processes, afforded by these new imaging techniques, have given rise to a host of new questions regarding the orchestrating mechanisms underlying complex signaling events, the answers to which require precise perturbations that induce very specific and controlled changes.

Given the complex spatial organization of the cell cytoplasm and the strict temporal order of molecular signaling events, traditional experimental methods to probe and dissect cellular signal transduction suffer from major drawbacks. Light-gated protein modules and other molecules offer both spatial and temporal control of proteins' subcellular localization and functions. Recent years have witnessed a rapid expansion of these technologies which have already begun to produce spectacular advances in the understanding of cell biology, animal physiology, and behavior.

This thesis is written in two parts. The first part, consisting of one chapter, gives an overview of the current light-gated technologies to control protein functions. The second part which is divided in two separate chapters describes the development and testing of two novel technologies that make use of light to control cell surface receptors activation in a spatiotemporal specific manner. These chapters will also discuss the potential applications of these technologies to address outstanding questions in cellular signal transduction.

BIOGRAPHICAL SKETCH

Thinh Nguyen Duc has a Bachelor of Science degree, with honors, in Biological Sciences from Stanford University. He also holds a Master of Science degree in Management Science and Engineering specializing in Biomedical Enterprises from Stanford University.

Công Cha như núi Thái Sơn

Nghĩa Mẹ như nước trong nguồn chảy ra.

ACKNOWLEDGEMENTS

First and foremost, I thank my advisor Dr. Morgan Huse. This thesis would not have been possible without his mentorship. Morgan's patience, boundless energy and insightful mentorship have made the last five years a rewarding adventure. I am most grateful for the fact that Morgan values the intellectual development and the personal well-being of his graduate students equally. I am fortunate to have been his mentee.

I am grateful to all the members of my thesis committee Dr. Minkui Luo, Dr. Howard Hang and Dr. Tarun Kapoor for their invaluable advice and kind support throughout.

The Huse lab is a wonderful place to be a graduate student in no small part because of the kind, funny and most generous post-docs and graduate students that I have had the good fortune to call friends. Xin and Roshni, thank you for all the lunches and dinners we shared. You simply were the best lab mates I could have hoped for. To Preeni, thank you for being my lab Mom. To all the current and past members of the Huse lab, thank you for your kindness and the many laughs we shared.

My interest in science began in high school and was nurtured throughout college by numerous teachers and mentors. I am forever thankful to my high school science teacher Mr. William Lernard for instilling in me a curiosity and love for biology and chemistry. I would like to thank Dr. Margot Paulick who took me on a freshman in college. She was an extraordinary mentor who handheld me through my first silica column and taught me what a negative experimental control meant. I would like to thank Dr. Matthew Bogyo for

allowing a young undergraduate student to tinkle and run free in your lab with little supervision and for introducing me to the field of chemical biology. To all the postdocs in the Bogyo lab, in particular Montse, Jiyoun, and Aimee, you were simply inspirational to a young undergraduate researcher.

Graduate school is an incredibly lonely experience. I am fortunate to have had the most wonderful and supporting friends. To Cesar, you are my Chrysler building. Tiffany and Vince, I am so thankful to have met you in New York. You are the kindest people I know. To the best two-person household in lower Manhattan, Tammy and Brenden, some of my best New York memories were created with you. Lyniese, you and I have a date with LineNiece. To my Gavilan fruit flies, Sarah, Ping, Wendi, Nisha and Zach, I “g-love” you all very much. To all of my friends in NYC, I am thankful to have met the smartest and most vibrant group of people that you are.

To my best friend Nghi Nguyen, you were there when I got uniformly rejected by 12 different graduate programs. You were there for every single western blot and imaging experiment that went south. And you were there for every K-town food therapy appointment. For that and so much more, I thank you.

Overt displays of affection and gratitude are not very Vietnamese. And so betraying my upbringing, I would like to thank my family. To my older brother and sister-in-law, thank you being 3000 miles away yet never once far from my side. To my parents, for the son and daughter, the teachers, the humanitarians, and the most loving mother and father that they are, this thesis is dedicated to them.

TABLE OF CONTENTS.

LIST OF FIGURES

LIST OF ILLUSTRATIONS

CHAPTER1: A review of current methodologies to control protein functions with light.

Proteins are macromolecules that are the workhorse behind most cellular processes. They have a wide range of functions from providing structural support to enzymatic reactions and catalysis that support a cell's survival and propagation. In the cellular milieu, a protein's function is tightly regulated by complex mechanisms that involve cascades of regulators and effectors interacting in a precise spatial and temporal manner. In order to understand protein functions and in effect biological processes at a molecular level, precise control of protein activity is important. Light is an ideal external perturbation stimulus as light irradiation can be tuned in a spatial and temporal fashion. In recent years, there have been numerous light-gated technologies to control protein function. These technologies fit into three broad groups of approaches (1) Photocaged Small Molecules and Protein Ligands, (2) Chemical and Genetic Hybrids and (3) Genetically Encodable Light Responsive Proteins. The distinguishing factor between these categories is the type chemistry involved in the preparation of each technology. Photocaged small molecules and protein ligand approaches employ organic chemistry to covalently modify the relevant elements with photosensitive moieties. Chemical and genetic hybrid approaches combine genetic engineering and cellular expression of effector proteins. Protein function then is controlled with photo-sensitive elements which can be installed onto effector proteins *in situ* using biorthogonal chemistry, or supplied exogenously in the forms of synthetic photo-caged small molecules that activate or inhibit the effector protein. Finally, genetically encodable light

responsive proteins approaches are those that do not rely on any chemical modification and the light sensing elements are genetically encoded. In this chapter, I will attempt to give a broad overview of the technologies in each category.

1.1 Photocaged small molecules and ligands.

1.1.1 Photocaged small molecules.

Some of the earliest attempts to control protein function and cell signaling with light involved chemically installing on small molecules, at positions that are critical to the molecules' bioactivity, photo labile groups. This strategy relies on the chemical accessibility of the small molecules to be conjugated. As small molecules are often soluble in aqueous solution and can diffuse across the cell membrane, caged compounds that have known effects on effector protein function can provide a means to temporally, and to lesser extent spatially due to free diffusion, control signaling events. Photocaging was not a novel concept in chemistry as caging moieties had been extensively used as protecting groups during organic synthesis. However, it was not until biologically active molecules were caged that idea of using photocaging as a way to spatiotemporally control signaling events gain appreciation as a useful experimental tool.

The earliest small bioactive molecules that were caged were photocaged analogs of the metabolite ATP[1] and the secondary messenger cAMP[2] , which were synthesized in the late 1970s (Figure 1.1). Since then caged analogs of a wide range of compounds from hormones to cell permeable ion chelators to enzyme inhibitors and neurotransmitters have been synthesized

and used for biological experiments[3]. These caged compounds have afforded biologists the ability to control a variety of cellular functions using light. Indeed, caged neuro-transmitters have been proven to be very useful in the field of neuroscience[4]. Live brain slices, for example, once immersed in caged neurotransmitters, such as caged glutamate, can be stimulated in a spatiotemporally specific manner with light to emulate complex neural activity[6,7]. Caged second messenger molecules like cAMP and diacylglycerol have successfully been used to activate signaling circuits in cell biology experiments to study growth cone turning [8] and the activation of kinase dependent signal transduction[9] respectively.

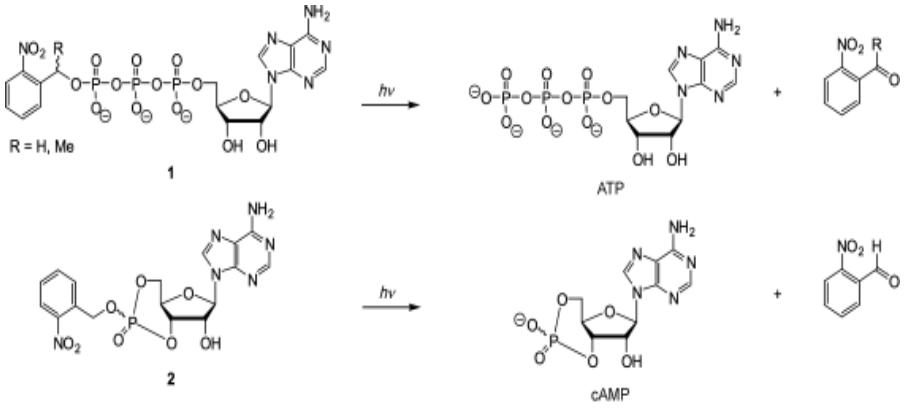

Figure 1.1: **Caged ATP and cAMP were two of the earliest photo-sensitive biologically active compounds to be synthesized.** Both compounds were modified with the UV-liable *ortho*-nitrobenzyl group. The synthesis and characterization of the *ortho*-nitrobenzyl analog of ATP in 1978 was where the term “caged” was first coined by the chemists involved[1]. Caged ATP is still commercially available today and applications of this compound are extensive[5].

1.1.2 Photocaged protein ligands.

Cell surface receptors constitute a large family of proteins that carry out the important function of sensing cues from the extracellular environment and translating those into cellular processes that affect function, growth and survival of the cell. Since many cell surface receptors bind to protein ligands, photo-caged protein ligands allow for the control of cell surface receptor activation with light. Furthermore, as ligands can be immobilized on solid surfaces, precise spatial control of receptor activation can be achieved as

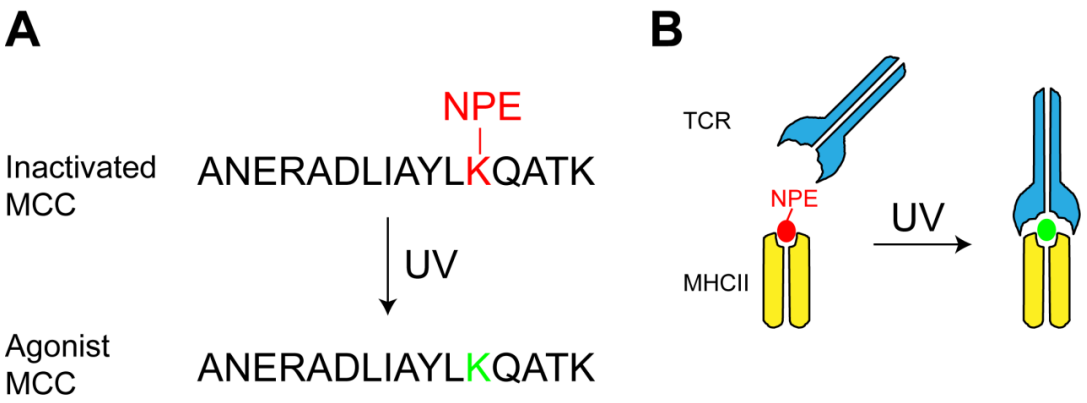

Figure 1.2: Photoactivation system to trigger TCR activation by UV light. (A) Caging strategy for the MCC peptide. A NPE group is attached to the lysine residue shown in red to inactivate the peptide. Subsequent UV irradiation cleaves NPE off the lysine and restores its native form (green). (B) Schematic graph of the photoactivation process. The large hydrophobic NPE group attached to the MCC peptide prevents the TCR from binding to the peptide MHC complex until it is cleaved by UV light. Figure adapted from Huse M., Immunity, 2007.

tethered decaged ligands cannot diffuse away from the local region of de-caging irradiation. Unlike small molecules, however, protein ligands present

unique challenges in terms of chemical modification. First of all, protein ligands are often large macromolecules. Ligands such as cytokines and growth factors can be tens of kDa in size and consist of hundreds of amino acids as is the case with the hormone Erythropoietin. Chemical syntheses of such large molecule are labor intensive and often low in yield. More challenging than the synthetic hurdle is the issue of where to attach the caging group. Protein ligands, unlike small molecules, are complicated molecules with secondary and tertiary structures whose structure-activity relationships are often unclear. This makes the task of engineering caged protein ligands whose activities are masked by a simple caging group difficult. Given said challenges, the development of caged proteins via direct chemical synthesis has lagged behind that of caged small molecules.

To date, the use of a caged peptide-major histocompatibility complex (pMHC) remains one of the more successful applications of photo-caged ligands. T-cell function is potently regulated by the activation of T-cell receptor (TCR) by the pMHC. One of the defining features of the pMHC complex is the presence of a short strand of peptide (which might be self or non-self in nature) that is “presented” by the MHC protein to the TCR. This particular composition allows for a caging strategy where a photosensitive group can be installed on an amino acid critical for TCR binding and activation (Figure 1.2). An MHC protein complexed with a caged antigenic peptide is able to control T-cell activation in a light dependent manner. When tethered onto solid surfaces, recombinant photo-caged pMHC can be used to control TCR activation with great precision[10,11]. This approach has been successfully used to perturb and delineate complex spatial and temporal

signal transduction downstream of TCR activation[12–14] as well as the inhibitory receptor KIR2DL2 involved in NK cells activation[15]. Clinically more relevant, caged pMHC forms the basis of conditional MHC technology[16] which is instrumental in transforming the synthesis of MHC tetramers into a more efficient process. Efficient recombinant MHC folding requires the presence of a strong binding target peptide sequence. MHC folding in the presence of a high affinity caged peptide allows for high yield production of pMHC complexes. The correctly folded pMHC containing the caged target peptide can then be irradiated in the presence of a high concentration of the target agonist peptide of choice. The caged peptide, upon UV-induced degradation diffuses away from the MHC binding cleft and is replaced by the target agonist peptide present in excess. This elegant technology has been used extensively to discover epitopes for important human diseases and to monitor the immune system in clinical settings[17].

Advances in peptide chemistry such as native chemical ligation and expressed protein ligation have made the synthesis and engineering of large polypeptides easier. Chemokines are generally small proteins of less than 100 amino acids and therefore are synthetically accessible via solid phase peptide synthesis with the aid of native chemical ligation when needed. Furthermore, chemokines are well-characterized in terms of their structures and functions. The N-termini of most chemokines, for instance, are unstructured and critical for chemokine agonist activity [18]. By installing a photosensitive moiety on critical amino acids in the N-termini of chemokines, one can control their activity with light. Chapter 2 of this thesis describes a

photocaged SDF1α chemokine and the application of this caged protein ligand in the study of chemokine receptor signaling.

1.1.3Chemical and genetic hybrids:

The direct chemical modification of bioactive molecules or polypeptide ligands with photosensitive moieties restricts the applicability of light-gated technology to the targets of these small molecules and protein ligands. By combining genetic expression and/or engineering with synthetic photoactivatable elements, hybrid approaches can be developed that expand the range of light-gated technologies. There are two general strategies to create hybrid technologies to control protein function with light: cis and trans-actuator (Figure 1.3).

Conceptually, trans-actuator technologies are simpler to design and implement. Trans-actuator hybrid technologies rely on the expression of effector proteins with domains responsive to chemical elements whose activity can be tuned with light. This strategy was first employed to generate approaches to control gene expression with great spatiotemporal precision. Transgene-based expression platforms, such as ecdysone[19] and doxycycline-based[20] systems, are great tools to control gene expression with the use of an exogenous agent. These systems make use of synthetic small molecules whose targets are gene-responsive elements able to drive gene expression. By caging the synthetic molecules, gene-expression can be controlled with light. Indeed, caged versions of ecdysone[21] and doxycycline[22] have been used to great effect to control gene expression in various

organisms (mouse embryos and *Xenopus laevis* tadpoles) with great precision by local irradiation with UV light or two-photon uncaging.

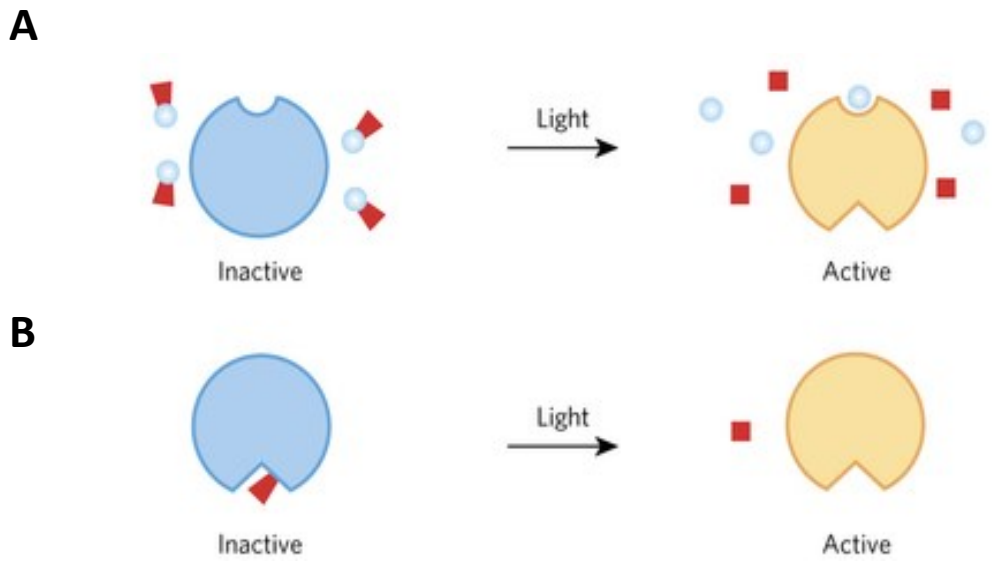

Figure 1.3: Trans and cis-actuator technology. (A) Trans-actuator technologies rely on expression of proteins containing domains responsive to photo-caged small molecules or elements supplied exogenously. (B) Cis-actuator technologies rely on the light-responsive elements being conjugated directly onto the proteins upon which they are to exert their light-dependent activity. Figure adapted from Gautier,A., et al., Nature Chemical Biology, 2014

Aside from transcriptional control of protein expression, trans- actuator technologies have also been developed to control protein localization and protein-protein interaction. A generalizable strategy to control protein-protein interaction utilizes a caged rapamycin molecule to control the heterodimerization of proteins that are conjugated to FK-506 binding protein (FKBP) and FKBP-rapamycin binding protein (FRB.) By localizing FRB to the

plasma membrane and conjugating the GTPase Rac to FKBP, light controlled membrane recruitment of Rac and subsequent actin polymerization was achieved[23]. The FKBP domain can also serve as an inhibitory module and when conjugated to a kinase enables the control kinase activity with light[24]. A closely related technology to direct protein localization with light makes use of caged 4-hydroxyl-tamoxifen or cyclofen and the ligand binding domain of estrogen receptor (ER^{T2}). In the absence of ligand, ER^{T2} is sequestered by its cytoplasmic chaperone heat-shock protein (HSP) in a complex. This complex dissociates upon the binding of 4-hydroxyl-tamoxifen or cyclofen to ER^{T2}. By fusing effector proteins to ER^{T2}, lighted technologies have been developed to control nuclear protein localization[25,26] and DNA recombination in mammalian cells[27] with light.

Providing even more degrees of control, trans-actuator technologies that make use of plant-based phytochrome B (PHYB) and phytochrome interacting factor (PIF) have the added advantage of reversibility. Discovered as the protein that controls seedling stem elongation in *Arabidopsis thaliana*, PHYB, when expressed and bound to the chromophore PCB, is activated by red light (650nm) and inactivated by infrared light (750 nm)[28]. PHYB, in its PCB bound state, undergoes a conformational change when activated by red light and binds to PIF within seconds[29]. Taking advantage of this light dependent reversible dimerizing property, the PHYB-PIF system has been used to develop light-gated modules to control a wide range of signaling events. The general strategy entails fusing an effector protein to the PHYB subunit and a corresponding regulatory element to the PIF subunit. After supplying the cell with PCB, light can be used to force interaction between

an effector protein and its regulatory element. For example, the PHYB-PIF system was used to control actin polymerization by forcing interaction between the small GTPases Rac[30], CDC42[30], Rho[30] and the corresponding GEFs. Activation of the lipid kinase PI3K was controlled with light by forcing interaction between the kinase catalytic domain and a membrane bound activating domain of a PI3K regulatory protein[31].

Cis- actuator technologies, which rely on the photosensitive elements to be conjugated onto the protein upon which they are to exert caging function, are technically more challenging. The caging element has to be installed onto the protein of interest at a specific location. Some of the most successful cis-actuator platforms have been those developed for the control of ion channels (Figure 1.4). The general strategy makes use of a photo-isomerizable azobenzene moiety conjugated to a bulky and charged quaternary ammonium group. This moiety adopts a cis configuration when irradiated with high energy light (380nm) and a trans configuration when irradiated with lower energy light (500 nm.) When tethered just above the pore of an ion channel, the trans configuration, which is 7 angstrom longer than the collapsed cis configuration, can extend over the pore and blocks ion exchange with the positively charged and bulky quaternary ammonium group. In practice, the modification of ion channels *in vitro* as well as in live cells is carried out with a maleimide conjugated azobenzene moiety. The maleimide forms a covalent bond with thiol group on the side chain of a solvent exposed cysteine residue which has to be introduced into the ion channel of interest as a point mutation. Using this approach, a light gated K+ channel was generated[32]. Light-activated ionotropic glutamate receptor[33]

and potassium-selective glutamate receptor[34] were also developed by switching out the quaternary ammonium group with a glutamate analog.

The ease by which light-gated ion channels were modified *in situ* using a maleimide warhead is an exception to the often complicated problem of chemical derivatization of proteins. Codon suppression technology, which allows for the introduction of unnatural amino acids into proteins with engineered tRNAs, has largely circumvented the technical challenges involved when modifying proteins with photosensitive elements in a site-specific fashion. Indeed, codon suppression technology has been used to develop light-gated tools to control a range of biological processes. For example, methods to control protein localization[35] and gene expression[36] were developed by replacing critical lysine residues in the nuclear targeting sequence (NLS) of effector proteins or in the promoter binding domain of polymerases respectively with photoactivatable lysine analogs. Kinase signal transduction[37] and cysteine protease activity[38] were similarly controlled by replacing, respectively, phosphorylation target tyrosines and catalytic cysteine residues with light-sensitive analogs. As the codon suppression technology continues to improve to allow for the incorporation of unnatural amino acids into effector proteins at the organism level, light-gated technologies are set to expand in the types of biological processes that could be modulated with spatial and temporal specificities.

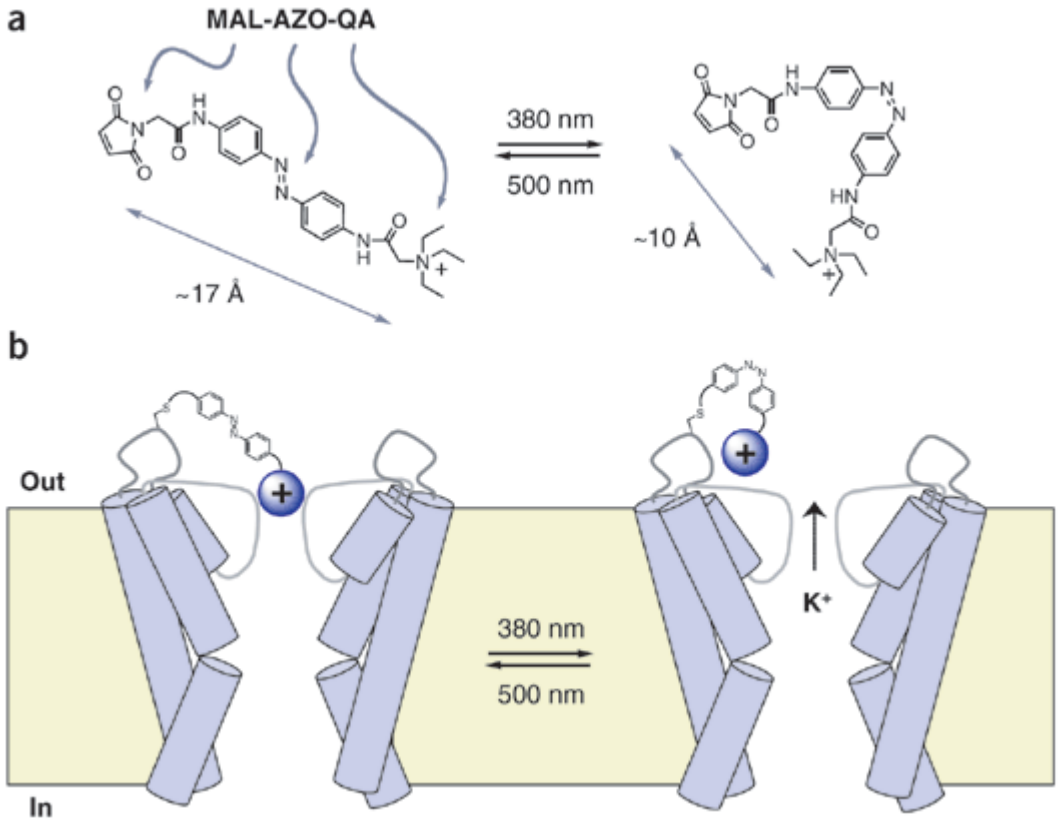

Figure 1.4 A light-gated ion channel as an example of a cis-actuator technology. (A) Chemical structure of the photo-isomerizable azobenzene. The maleimide (MAL) "warheard" allows for covalent modification at cysteine residues that have been introduced via point mutation. The azobenzene (AZO) is the light responsive element that photo-switches between trans and cis conformation whose difference in length provides the blocking or caging of the ion channel. The quaternary ammonium (QA) group, which is interchangeable with other functional groups depending on the target ion channel, is in this case specifically chosen for its positive charge to keep out cations. (B) Caged potassium channel in action. Figure adapted from Banghart, M. et al., Nature Neuroscience, 2004.

1.2 Genetically Encodable Light Responsive Proteins

The last category of technology includes some of the most recent advances in the use of light to control protein function. These technologies rely on genetically encoded protein actuators that change conformation and become activated in response to light. By repurposing these proteins either through engineering or hi-jacking their natural function by expressing them in non-native cells or organisms, genetically encoded light-sensitive proteins have the distinct advantage of being a single component system, eliminating the need to exogenously supply light responsive molecules. This single component property is important particularly for organism-level control of protein function where the exogenous delivery of a synthetic photo-sensitive cofactor might be technically challenging or physiologically traumatic.

The earliest genetically encoded light-gated technologies were developed from opsins which are photoreceptors that sense light as a stimulus. These proteins require the presence of a vitamin-A related cofactor called retinal to function. In their retinal-bound forms, opsins are referred to as rhodopsins. Because retinal is present at sufficient concentration in most mammalian tissues, opsin proteins can function when expressed in mammalian cells without the need to supply the co-factor[39]. There are two broad families of opsins: microbial opsins (type I) and animal opsins (type II). The two families of proteins, which share very little sequence homology between their members, all encode 7-transmembrane receptors. Microbial opsins which control a wide range of functions in bacteria and fungi have been adapted to control neuronal activity in mammalian cells and whole animals. For

example, bacteriorhodopsin, which is a light sensitive proton pumps, halorhopsin, which is a light-sensitive chloride ion pump and chanelrhodopsin, which lets cations across the membrane in response to light, have all been expressed in neurons and whole brains. They have enabled researchers to, in a light dependent manner, hyperpolarize neurons and control neurological activities[40,41]. These technologies have led to unprecedented new understandings of neuronal circuitry and cognition[42]. They have also been adapted for the control of cardiac functions[43] using light and for tracking stem cell development[44].

Animal opsins, which are predominantly G-protein coupled receptors (GPCRs), have been the subjects of intense structural studies. Such efforts and the resulting knowledge have allowed for the engineering of functional chimeric GPCRs where the extracellular and transmembrane domains of animal opsins are fused to the intracellular domain another GPCR. Such chimeras, referred to as OptoXR[42], are light-sensitive receptors whose activation can be controlled with great precision (Figure 1.5). For example, bovine rhodopsin has been fused with β-adrenergic, α-adrenergic and serotonin (5-hydroxytryptamine (5-HT) receptors to create chimeric GPCRs that when expressed in the brain allow for the control of animal behaviors in a light-dependent manner[45]. Recently, by fusing bovine rhodopsin to the chemokine receptor CXCR4, a photoactivatable chemokine receptor was developed that permits for light-gated control of chemotaxis *in vitro* as well as recruitment of lymphocytes to tumor sites in a mouse using light[46]. GPCRs, as the largest and most diverse family of cell surface receptors, control numerous critical physiological processes ranging from sensory

functions, to the regulation of the immune system to cancer pathogenesis. That OptoXR is an elegant and effective strategy for light-gated control this family of receptors is scientifically exciting and clinically relevant.

Also from a bacterial source, photoactivatable adenylyl cyclases (PACs), which are light sensitive receptors that transduce cAMP signaling to control photoavoidance in soil bacteria[47], have successfully been used to control cAMP signaling in a light dependent manner in mammalian cells[48]. PACs, similar to opsins, make use of a co-factor, flavin adenine dinucleotide (FAD), that is ubiquitous in the cellular environment, and therefore function as single component light-gated platforms. Unlike opsins however, PACs suffer from high background activity in the dark as well as poor expression and in vivo folding[48] and so therefore have not been used widely.

Photo-sensitive receptors, as discussed, are great tools to engage the full complement of signal transduction involved in regulating a particular cellular process. Naturally occurring light-responsive cytoplasmic proteins have also played important roles as building blocks for light-gated technologies. As reviewed in 1.2, PHYB-PIF based technologies have enabled researchers to control of protein functions via light-inducible dimerization. The drawback of the PHYB-PIF platform is the need to supply the cofactor PCB by either directly supplementing the cell culture medium or expressing the relevant enzymes to synthesize PCB in the cell of interest. Fortunately, there are other photo-sensitive cytoplasmic proteins derived from plants and coral such as cryptochrome 2 (CRY2), light oxygen-voltage (LOV) protein domains, the fluorescent protein dronpa and cytoplasmic UV-B detecting

receptor (UVR8), that do not require cofactors. These proteins form the foundation upon which numerous light-gated technologies have been developed.

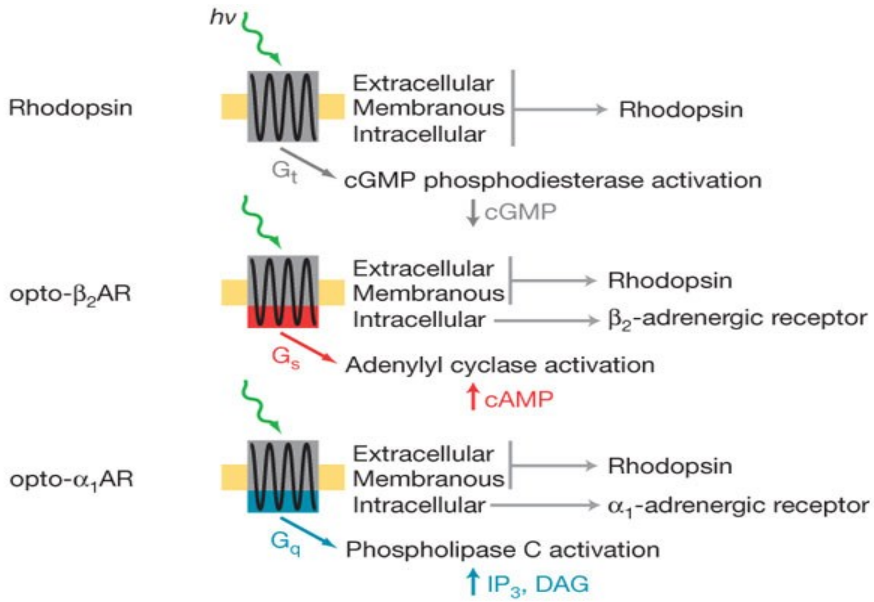

Figure 1.5 Chimeric GPCRs engineered from light-sensing rhodopsins are genetically encodable light-gated technologies. Decades of structural studies of mammalian opsins have provided detailed understanding of the allosteric circuits underlying the light-sensing property of these GPCRs. This knowledge enables the engineering of functional chimeric receptors containing the extracellular light-sensing domain of rhodopsin and the intracellular signal transduction domains of other GPCRs. These light-responsive GPCRs termed OptoXRs provide researchers with unprecedented spatiotemporal control of the most diverse and functionally important class of cell surface receptors in eukaryotic organisms. Figure adapted from Airan, RD., et al., Nature (2009).

Cryptochrome 2, expressed in Arabidopsis thaliana, is a blue-light sensing protein that uses the ubiquitously expressed flavin as the photon-sensing chromophore. Upon illumination, CRY2 homo-oligomerizes and binds to its cognate partner, the cryptochrome-interacting basic helix-loop-helix domain (CIB1) within seconds[49]. When illumination is withdrawn, CRY2 reverts back its monomeric and inactivated form within 5-10 minutes[50]. This light-sensitive oligomerization property has been exploited to control a wide of range of protein functions and cellular processes. When the CRY2/CIB1 proteins are conjugated to split subunits of a transcription activator protein (GAL4) or a DNA recombinase (CRE), light-induced oligomerization of the CRY2/CIB1 complex provides a means to control gene expression and DNA recombination events respectively[51]. Using a slightly different strategy than the split effector proteins approach, by fusing the CRY2 protein to either a customizable DNA promoter binding protein TALE or an inactivated endonuclease Cas9; and the CIB1 protein to a transcription activator, remarkable optical control of mammalian endogenous transcription and epigenetic states has been achieved[40]. Not limited to just gene expression control, the CRY2-CIB1 system has been used to develop methods to control other effector protein functions via light-inducible clustering. After conjugating CRY2 to the multimeric protein CaMKIIα and CIB1 to an effector protein, illumination with blue light causes cytoplasmic clustering of the effector protein and as a result modulates its activity. This strategy was employed to control with light the activity of Vav, a Rho-GTPase GEF that controls membrane ruffling, and the lipid kinase PI3K[52]. Finally, the protein CRY2 alone, which as discussed, homodimerizes upon blue light irradiation,

has been used to control cell surface receptors activation via optically controlled dimerization[53,54].

Even more extensively used in light-gated technologies than CRY2, is the light-oxygen-voltage (LOV) domain family of proteins, which was first discovered to mediate phototropism in plants. LOV domains are the photo-reactive modules that sense blue light and convert this stimulus into a myriad of signaling responses[55]. Proteins that contain LOV domains are diverse in structure and function and are present in plants, bacteria and fungi. LOV domains themselves are therefore also very structurally diverse. There are however a few common features tying the family together. LOV domains tend to be around one-hundred amino acid long, forming a Period-ARNT-Singleminded (PAS) domain that binds a flavin chromophore[56]. There is also the presence of a consensus GXNCRFLQ motif[57]. Upon blue-light irradiation, LOV domains form a covalent linkage with the bound flavin cofactors, which leads to a series of allosteric conformational changes that regulate the parent proteins' function (Figure 1.6). This process is reversible in the dark with kinetics that range from minutes to days that can be tunable via mutagenesis[58]. The precise mechanism and conformational changes upon irradiation differ subtly but significantly among the different LOV domains. This diversity has provided researchers with a rich toolkit from which to build light-gated technologies to control protein functions in a variety of settings. Generally, there are two main strategies to create light-gated technologies using LOV domains. The first strategy involves conjugating an effector protein to a LOV domain via a helical linker which acts an inhibitory element to the protein's function. Conformational changes in the LOV domain upon

blue-light irradiation release the inhibitory linker and restore the function of the effector protein. The second strategy, which is more frequently used, exploits blue-light induced homo-dimerization of certain LOV domains. Similar to the CRY2-CIB1 or PHYB-PIF based technologies; light-gated technologies can be created by fusing split effector proteins or complexes to LOV domains (Figure 1.7).

Currently LOV-domain based technologies use one of five LOV domains which include a LOV domain of phototrophin 1 in the plant *Avena sativa* called AsLOV2[59], a photoreceptor found in *Neurospora crassa* that regulates circadian rhythm called vivid (VVD)[60], a component of the *Bacillus sublitis* stressosome (YtvA)[61], an output component responsible for the transition to flowering called flavin-binding, kelch repeat, F-box 1 (FKF1)[62], and a LOV-domain containing transcription factor present in *Eyrothobacter litoralis* called EL222[63].

More recently, the protein dronpa, which was first identified in the coral Pectiniidae, has been used to develop light-gated technologies. Classically known as a green fluorescent protein with great photo-stability and brightness that is reversibly photo-activated upon irradiation[64], dronpa also undergoes light-driven dimerization when irradiated with a 390 nm that can be reversed with a 490 nm light [65]. Capitalizing on this reversible dimerization property, one strategy to create light-gated technologies involves fusing one copy of dronpa each to the amino and carboxyl termini of an effector protein. When irradiated with 390 nm light dronpa dimerizes and inhibits the effector protein function by morphing its conformation. Upon

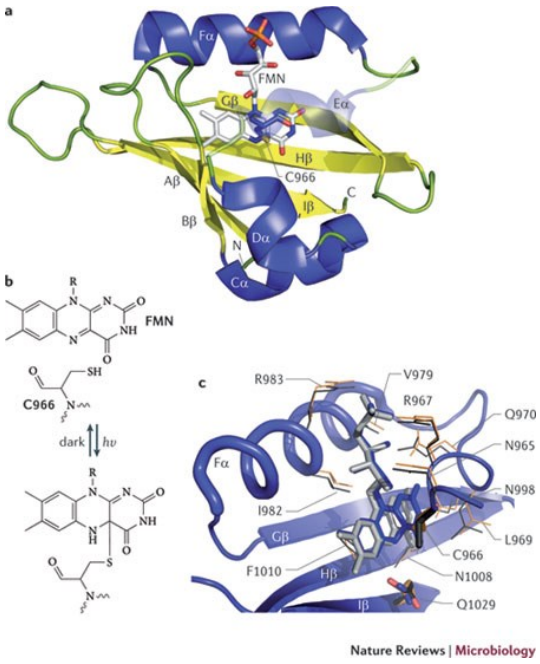

Figure 1.6 LOV domain containing proteins belong to a large and diverse family of light-sensing proteins that use flavin mononucleotide (FMN) as the photosensitive chromophore. (A) Structure of an "activated" LOV2 domain. The (FMN) cofactor in gray is shown to be in covalent complex with C966. (B) A schematic showing the covalent interaction between C966 and FMN upon blue light irradiation. (C) The FMN-binding pocket of the LOV2 domain. Residues that interact with the FMN cofactor are shown in either orange for the illuminated state or in grey for the dark state. Key residues of the highly conserved motif GXNCRFLQ shared among LOV domains are labeled. Figure adapted from Herrou, J., et al., Nature Review Microbiology (2011)

irradiation at 490 nm, the dronpa dimer is disrupted and the target protein's

function is restored. Using this strategy, optical control of cytoskeletal dynamics and protease function were achieved with great spatial and temporal resolution[66].

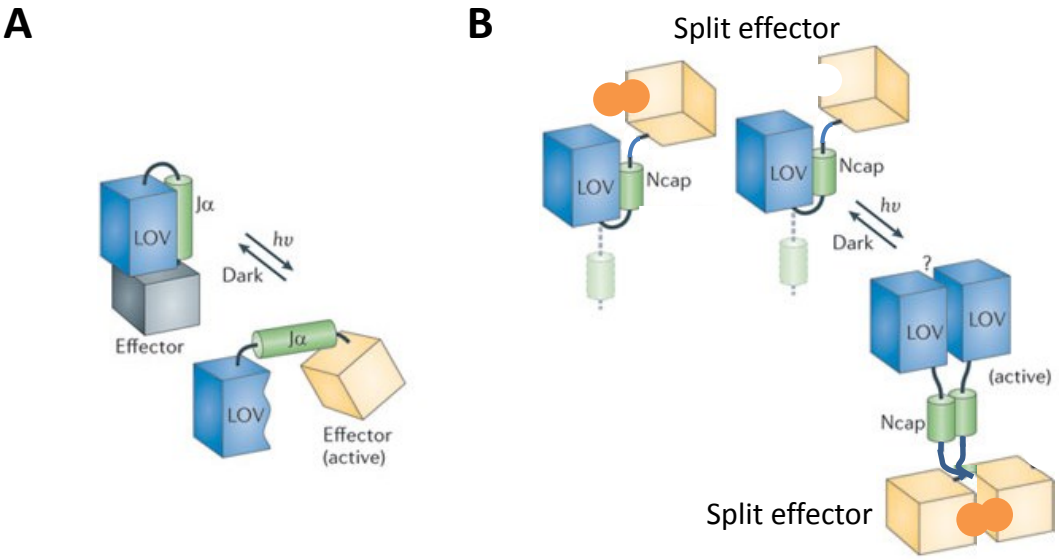

Figure 1.7 Two general strategies are employed to create light-gated technologies to control protein function using LOV domains. (A) A LOV domain and an effector protein are conjugated via a helical linker which acts an inhibitory element to the effector protein's function. Conformational changes in the LOV domain upon blue-light irradiation release the inhibitory linker and restore the function of the effector protein. (B) Some LOV domains undergo light induced dimerization. Light-gated control of an effector protein can be achieved by conjugating the split effector protein to LOV domains. Figure adapted from Herrou, J., et al., Nature Review Microbiology (2011)

Finally, as the most recent addition to the rapidly expanding family of photo-sensitive proteins isolated from plants, UVR8 is unique in that it detects and

responds to UV-B light[67,68]. In its “inactive” form UVR8 exists as a dimer and upon UV-B irradiation, within seconds, monomerizes. The monomers can themselves revert to dimers albeit with a slow kinetics on the time scale of hours[69]. This property has been exploited to control protein secretion in mammalian cells. The strategy involves conjugating multiple copies of UVR8 to a protein that would normally be secreted. Without UV-B irradiation, the effector protein, driven by UVR8’s default state of dimerization, aggregates and cannot be secreted. Upon irradiation, the monomerization of the attached UVR8 allows for the detachment of the effector protein and synchronized light-controlled secretion is achieved[70].

1.3 Discussion

It is clear that light-gated technologies have provided scientists with remarkable tools to answer important questions across biological disciplines. Neurobiologists have seen the impact of these technological advances, termed optogenetics by researchers in the field, in the most significant way. Optogenetics has allowed for unprecendented perturbation and control of processes such as memory formation, depression and cognitive functions previously deemed impossible to manipulate experimentally. The advent of optogenetics played no small part in the recent multimillion dollar BRAIN initiative by the US government to map and understand the brain better. A few reasons underscore the success of optogenetics in neurobiology. Opsins, which were used to develop optogenetics, have relatively rapid photocycles in the range of 10-20 ms[39] which allows for sufficient temporal control of neuron depolarization. From the spatial resolution perspective,

optical control of neuronal circuits and behaviors rests on the control of groups of cells rather individual cells or subcellular compartments of a neuron. This, coupled with advances in viral transduction, enables spatial control of neuronal activity with sufficient experimental resolution. Lastly, the open source approach of the original investigators, who started the field of neuro-optogenetics, to disseminate the techniques has played an important role in the wide adoption and usage of the technology among neurobiologists.

Cell biology and the study of signaling pathways that underlie cellular processes in response to stimuli from the environment stand next to gain in the same way that neuroscience has done from light-gated technologies. There are however several outstanding issues. Most importantly, perturbations to dissect signaling in cell biology require subcellular spatial resolution. With recent advances in two-photon microscopy and other optical instrumentation, it is possible to focus light to illuminate geometrically defined regions inside the cell. However, the practical spatial resolution of a photoactivatable actuator will match the resolution provided by the focused light source only if the photo-activated element does not diffuse in the cell in the timescale that researchers would like to observe certain signaling processes. This is particularly problematic for caged small molecules whose spatial specificity is limited by the rate of free diffusion in the cellular milieu. Genetically encoded photosensitive proteins also suffer from the same issue though in some cases there are effective, but technically challenging, workarounds. Systems that use the PHYB-PIF complex, for instance, to optically control protein function have the advantage of full-reversibility that

allows for precise spatial control of activation. As PHYB-PIF is rapidly activated by blue light and just as rapidly inactivated by far-red light, by superimposing localized red light over a uniform field of far red light, researchers with significant technological capability and instrumentation at their disposal, can achieve spatial control. It is worth noting that this strategy only works for the PHYB-PIF system. The most frequently used photo-sensitive proteins such CRY2 and LOV domains once activated undergo a much slower (5-10 seconds for CRY2 and 10 to 10000 seconds for LOV domains[58]) thermal reversion to the inactive states. Precise spatial control therefore remains an issue to be addressed.

As aforementioned in 1.1.2, photo-caged extracellular ligands when immobilized on solid surfaces can provide precise spatial control of cell surface receptor activation as the tethered ligands, once decaged locally by focused irradiation, cannot diffuse away. Our laboratory pioneered two of such techniques to activate the TCR and the inhibitory NK cell receptor KIR2DL2. When coupled with high magnification live cell imaging, these tethered extracellular ligands have enabled very precise spatial stimulation of immune receptors. The TCR and KIR2DL2 both recognize short agonist peptides which are bound and “presented” by larger major histocompatibility complex (MHC) proteins. The design and synthesis of photo-caged ligands for these receptors therefore involve modifying short peptide sequences, which can be readily synthesized via solid phase peptide synthesis, with caging groups on residues known to be critical to the peptides’ agonist activity. Chapter 2 of this thesis describes an effort to extend this caged ligand strategy beyond the caging of short polypeptide chains. It describes

the design and synthesis of a full-length caged chemokine protein that allows for the precise spatial and temporal control of chemokine receptor signaling. Chapter 3 gives an account of the development of a “universal” photo-caged extracellular ligand able to control with high spatial precision the activation of a range of cell surface receptors.

CHAPTER 2: Development of a photoactivatable CXLC12/SDF1α for the study of CXCR4 signaling in lymphocytes.

2.1 INTRODUCTION:

2.1.1 Lymphocyte migration and motility

T-lymphocytes or T-cells are a critical component of the adaptive immune system. T-cells possess highly agile migratory capabilities which are essential to their development and function as effectors in the clearing of infections[71]. Differentiated from hematopoietic stem cells in the bone marrow, T-cell progenitors migrate out of the bone marrow into the thymus for extensive selection and maturation[72]. Mature yet naïve T-cells only respond to infections when their T-cell receptors (TCR) recognize antigens. Since T-cells develop in the primary lymphoid organs, namely the bone marrow and the thymus gland, and antigen present cells (APCs) which detect and present antigens for TCR engagement reside in secondary lymphoid organs (lymph nodes) at different locations throughout the body, T-cell migration to and from lymphoid organs is critical to their function[73]. After activation, antigen-specific T-cells have to migrate and scan the body to find sites of inflammation and disease to perform their effector functions[71]. Once infections have been cleared, some memory T-cells migrate or home to specific regions of the tissue in order to mount a rapid response in case of future repeated infections[74].

T-cell migration is associated with a specific migratory morphology (Figure 2.1). This structural configuration, which resembles a hand-mirror, consists of a broad, actin-rich lamellipodium at the leading edge followed by a

cylindrical uropod at the rear. T-cell migration uses a mechanism mirrored by the amoeba *Dictyostelium discoideum*. Four distinct steps coordinate the forward movement of the cells: actin dynamics drive the formation of protruding pseudopods, the protruding membrane and associated receptors sense the extracellular environment by interacting with ligands and substrates, myosin-based contractibility squeezes the cell body in the mid-region, and the rear end of the cell moves forward propelling directional movement[71]. T-cell migration is a special kind of cell movement compared to mesenchymal or epithelial migration. First of all, T-cell migration is fast with speed up to 30 μm/min[75]. T-cell migration also does not promote the formation of strong adhesion to surrounding tissues. These two unique properties make T-cell migration one of the most dynamic forms of cell migration.

2.1.2 Chemokines and their receptors

T-cell migration is highly directional and is regulated by chemokine receptors and chemokine ligands. Chemokines compose of a family of small, di-sulfide-linked proteins that are produced and secreted by endothelial and epithelial cells as well as leukocytes[76]. Chemokines transmit signal by engaging specific G-protein coupled receptors (GPCRs). Different tissues express different sets of chemokines which help differentiate populations of T-cells that migrate to or get “recruited” to particular body sites. Chemokines can be either inflammatory or homeostatic[77]. Inflammatory chemokines, which are produced and secreted during pathological conditions such as

bacterial or viral infection and malignant tumor development, help recruit immune cells to sites of disease.

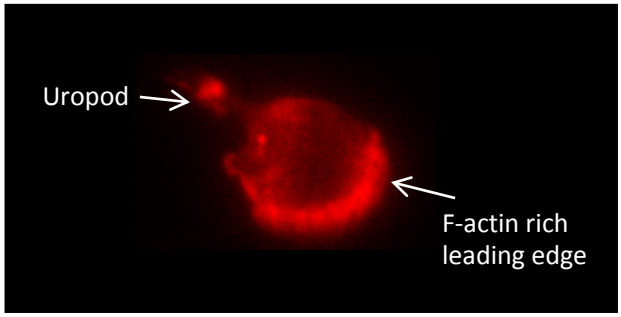

Figure 2.1 Immunocytochemical staining of F-actin (in red) of a migrating primary mouse T-cell. The anterior-posterior axis is clearly marked by the differential accumulation of F-actin in the protruding lamellipodia at the front and the stalk-like uropod structure at the back.

Inflammatory chemokines, which are produced and secreted during pathological conditions such as bacterial or viral infection and malignant tumor development, help recruit immune cells to sites of disease. Homeostatic chemokines are mainly found in lymphoid organs and help maintain leukocyte homeostasis and development in these organs[77]. Aside from functional distinctions, four subtypes of chemokines based on structural features have also been categorized. C, CC, CXC and CX_3C denote the number and spacing of cysteine residues in the amino-terminal region of the chemokine. All of the subtypes except for the CX_3C family, which has a transmembrane and cytoplasmic domain, are secreted proteins[76]. Chemokines activate their receptors in a two-step mechanism[18]. First the globular portion of the chemokine binds to the receptor. Then, the N-terminal tail of the chemokine induces a conformational change in the receptor's

transmembrane helices (Figure 2.2). This activates the associated G-coupled proteins, leading to PI3K signaling, calcium flux, cytoskeletal remodeling, and the enhancement of integrin-mediated adhesion[78]. These and other events drive the acquisition of hand-mirror morphology.

2.1.3 Polarization of cytoskeletal and signaling scaffolds downstream of chemokine receptor activation in T-cells.

The binding of chemokines to chemokine receptors triggers dramatic signaling and morphological changes in T-cells. At rest, T-cells show a symmetrical cell body that, upon exposure to a chemotactic agent transforms into a highly polarized migratory morphology within minutes. At the top of the signal transduction cascade is the dissociation of the heterotrimeric G-proteins consisting of αβγ subunits from the chemokine receptor upon ligand binding. Critical chemotactic signal transduction is then carried out by the Gβγ dimer which activates two major signaling circuits, phospholipase C and PI3K, initiating downstream signaling cascades[79]. At the bottom of these signaling cascades are highly compartmentalized signaling complexes that define and segregate the cell body into distinct regions. For instance, at the leading edge highly dynamic actin polymerization supports a protruding lamellipodia. Such cytoskeletal dynamics is driven by the Rho-GTPase Rac. The Rac-GEF DOCK2 has been shown to be an important regulator of this process[78]. In the mid-region, actomyosin signaling drives contraction the body and limits lateral protrusion[71,75]. The motor protein Myosin II which can cross-links actin filaments has been shown to be important for this process. While individual signaling components and pathways involved in chemotactic

response in T-cells are largely known or can be inferred from similar cellular systems, namely neutrophils and *Dictyostelium,* outstanding questions remain as to how these signaling circuits are propagated and integrated spatially and temporally from receptor activation at the plasma membrane to achieve morphological polarity and directional movement.

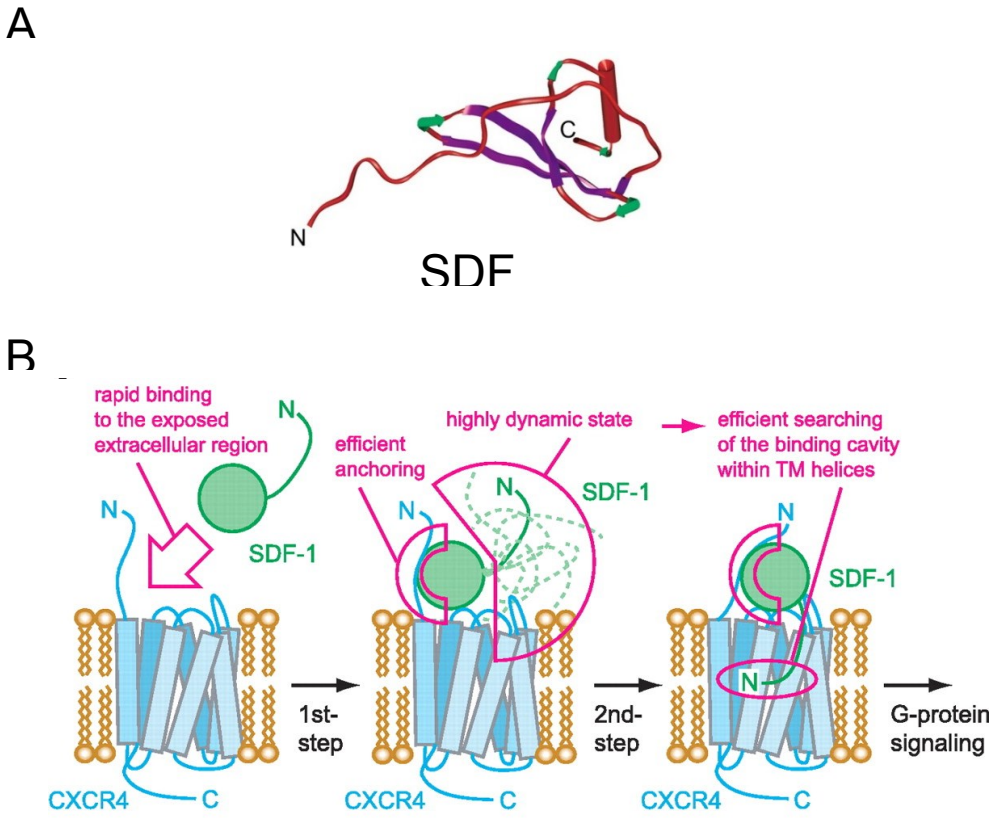

Figure 2.2 (A) Crystal structure of SDF1α show a long and unstructured N-terminus. (B) The two step mechanism by which chemokines (SDF1α shown) activate their receptor (CXCR4 shown). Figure adapted from Fernandez, EJ., et al., Annual Review of Pharmacology and Toxicology (2002) and Kofuku, Y., et al., Journal of Biological Chemistry (2009).

2.1.4 Current chemical biology tools for studying directed cell migration

The use of fluorescent proteins allowed for some of the initial observations and appreciation for the highly compartmentalized nature by which proteins and signaling components involved in chemotaxis are orchestrated inside the cell. Some but not all chemokine receptors, for instance, preferentially localizes to the front of a migrating cell. Other molecules such ERM adaptor proteins are localized exclusively to the trailing uropod[71]. Adding to the spatial complexity of these signaling events is the rapidity by which morphological changes occur. For example, chemokine stimulation induces rapid up-regulation of F-actin polymerization within seconds and ensuing signaling events completely transform the cell body within minutes into a migratory configuration[80]. Such spatiotemporal specificities in signal transduction have led to the development of chemical biology tools to perturb and dissect signaling downstream of chemokine receptors with high spatiotemporal resolution.

In contrast to conventional methods of perturbation such as genetic knockdown and small molecule inhibitors, chemical biology methods, particularly those that allow for optical control protein functions, provide greater control over the timing and location of a perturbation to a signaling circuit. A substantial amount of efforts has gone into developing methods that involve the microinjection of caged inhibitory peptides or caged proteins. For example, a caged peptidic inhibitor of myosin light chain kinase (MLCK) was developed, and after microinjection into eosinophils, was shown to halt locomotion in a UV dependent manner[81]. Another strategy involves semi-

synthesis via expressed protein ligation a caged Myosin II where a critical phosphor-serine residue was caged. When injected into cells, UV irradiation was able to restore the native phosphorylated protein[82]. Methods like these while elegant from a chemical engineering perspective are not useful to the extent that microinjection is necessary. There is also the issue of free diffusion which greatly limits the compartmentalization of the corresponding signaling once the microinjected effector proteins or inhibitory peptides are activated by light.

Methods to control chemotactic signal transduction that make use of genetically encoded photosensitive proteins are less invasive to the cells. The focus of these technologies for the study of chemotaxis has mainly revolved around the Rho-GTPases due to the fundamental role they play in cell migration. As reviewed in chapter 1, photosensitive versions of RhoA, Rac1 and cdc42 have all been developed with varying degrees and ease of spatial control[30]. It is important to note that these technologies only allow for the control of individual signaling pathways and not the full complement of signaling events downstream of chemokine receptor activation. The elegant photoactivatable CXCR4[46] solves this problem but again suffers from limited spatial control due to lateral diffusion of the receptor in the lipid bilayer plasma membrane.

We sought to develop a photoactivatable chemokine that would enable precise spatial and temporal control of the full complement of signaling downstream of chemokine receptor activation. A photoactivatable chemokine would have two distinct advantages. As an extracellular ligand, it

could be immobilized on solid surfaces, which ensures a sustained and local source of activation upon decaging. A second advantage would be that cells would not have to be modified genetically with chimeric receptors or microinjected with cage reagents.

2.2 RESULTS:

2.2.1 Design and synthesis of a photoactivatable CXCL12/SDF1α.

We chose to focus our efforts on developing photoactivatable SDF1α, which is also known as CXCL12. SDF1α is a prototypical chemokine that has pleiotropic functions. SDF1α knock-out mice are embryonic lethal. Not only is the chemokine strongly chemotactic to leukocytes, SDF1α has been implicated in the migration of metastatic cancer cells. SDF1α binds to two GPCR chemokine receptors CXCR4 and CXCR7[76,83]. From a structural stand point, SDF1α is an 8kDa protein consisting of 67 amino acids. The chemokine's amino-terminal domain consisting of 8 amino acids is highly disordered. Mutagenesis studies identify the N-terminal lysine residue to be of particular important to the agonist activity of SDF1α. Specifically, truncation of this lysine residue (SDF1α 2-68) or its replacement with another basic residue (SDF1αK1R) resulted in isoforms that are orders of magnitude less potent than the wild type protein[84]. The unique reactivity of the N-terminal lysine residue gave us a strategy to design a photoactivatable protein. By installing a photocleavable 4,5-Dimethoxy-2-nitrobenzyl (NVOC) moiety at the ε-amino position of the N-terminal lysine, we hypothesized that the agonist activity of SDF1α could be controlled using light (Sheme 2.1).

The small size of the chemokine makes it synthetically tractable via the use of solid phase peptide synthesis (see Materials and Methods). Using standard FMOC-peptide chemistry, we built the peptide chain on PEGylated Rink Resin support to aid solubilization and minimize chain collapse. The NVOC moiety was installed via the use of a commercially available FMOC-Lys(NVOC)-OH amino acid analog. After chain extension completion, the NVOC-SDF1α polypeptide was cleaved, purified and refolded to produce the caged chemokine (see Materials and Methods for folding protocol).

2.2.2 NVOC-SDF1α induces chemotactic response in a UV-dependent manner.

To test that NVOC-SDF1α behaves as a photoactivatable chemokine, we performed a transwell chemotaxis assay. Primary $CD8^+$ T-cells were stimulated with commercial SDF1α, NVOC-SDF1α or NVOC-SDF1α that had been pretreated with UV light. Whereas commercial SDF1α elicited strong chemotactic response, NVOC-SDF1α failed been pretreated with UV light. Whereas commercial SDF1α elicited strong chemotactic response, NVOC-SDF1α failed to generate a response above background level. UV-pretreatment to remove the NVOC-caging group completely restored the ability of the chemokine to induce chemotaxis. (Figure 2.3) Chemokine stimulation of T-cells induces strong calcium flux[18]. We therefore also tested NVOC-SDF1α in a FACS-based fluorometric calcium flux assay. Primary $CD8^+$ T-cells robustly fluxed calcium in response to stimulation with commercially available SDF1α.

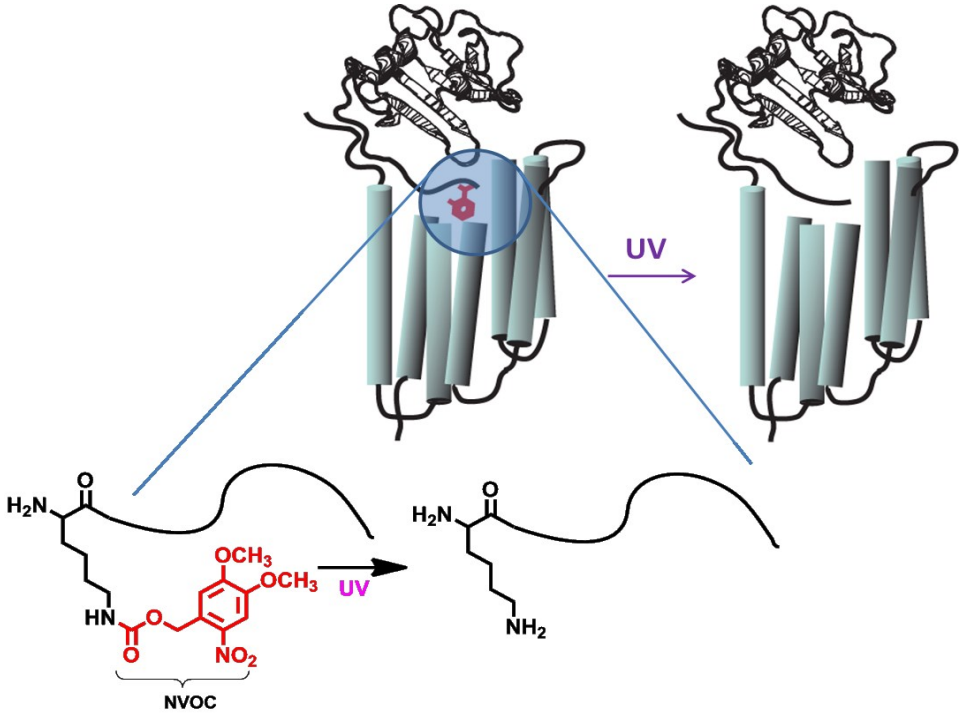

Scheme 2.1 Design of a photoactivatable SDF1α. The N-terminal Lysine residue of SDF1α is critical for its function. By installing a photo-cleavable NVOC group on the ε-amino group, caged SDF1α can be synthesized that would allow for the control of chemokine receptor activation (CXCR4) with UV light.

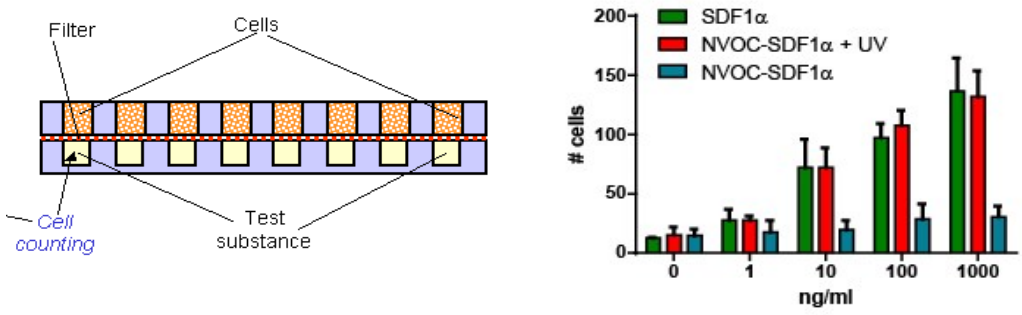

Figure 2.3 NVOC-SDF1α is able to activate CXCR4 in a UV-dependent manner in a transwell assay.

NVOC-SDF1α, however, only induced calcium flux when UV-irradiation was applied prior to stimulation (Figure 2.4). The transwell chemotactic assay and the calcium flux experiment demonstrated that NVOC-SDF1α is a photoactivatable chemokine able to stimulate its cognate receptor in a UV-dependent manner.

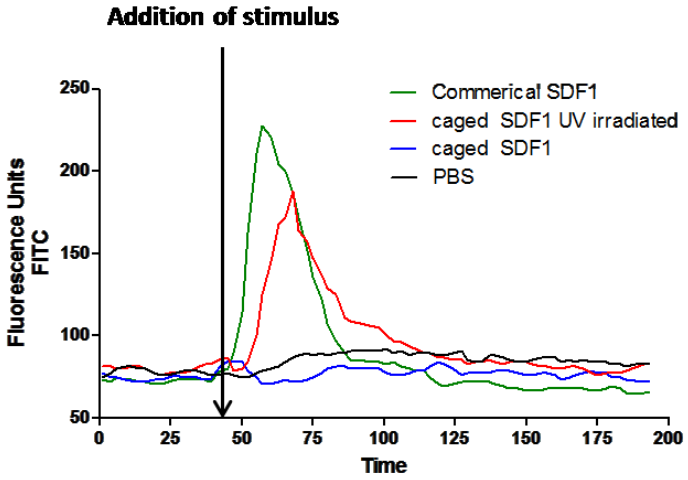

Figure 2.4 NVOC-SDF1α is able to activate CXCR4 in a UV-dependent manner in a fluorometric calcium flux assay.

Mouse T-cells loaded with a fluorescent calcium indicator are stimulated with chemotactic agents. Calcium flux is recorded using a flow cytometer. Increased fluorescence intensity in the FITC channel indicates an increase cytosolic calcium concentration. NVOC-SDF1α is unable to stimulate a response from primary mouse T-cells (blue line) unless irradiated with UV (red line.) UV irradiation completely restores the activity of the caged SDF1α to levels of commercial SDF1α (green line)

2.2.3 NVOC-SDF1α can activate CXCR4 with spatiotemporal specificity.

As the final test of our photoactivatable chemokine, we assessed whether the chemokine could be used to study chemokine receptor signaling in a live cell videomicroscopy experiment. Chemokine stimulation of T-cells induce a dramatic and rapid actin-cytoskeletal response[75]. In order to observe this response, we transduced Jurkat T-cells to express Wave2 conjugated to GFP. Wave2 is ubiquitously expressed in cells of the hematopoetic linage and acts downstream of the RhoGTPase Rac1 to promote actin polymerization in regions of cellular activation[85]. We adhered Jurkat cells expressing Wave2-GFP onto a glass surface coated with human fibronectin and NVOC-SDF1α. For these experiments, we used a Mosaic digital diaphragm system to deliver UV light to small regions on the surface beneath individual cells. Image acquisition was performed using a total internal reflection fluorescence (TIRF) microscope objective which allows for observation of signaling events occurring at and close to the plasma membrane. Upon photoactivation, Jurkat cells rapidly and robustly responded to local stimulation and directionally polarized their cell body (Figure 2.5A).Importantly, local irradiation of Jurkat cells on glass surfaces coated with fibronectin alone did not induce actin-cytoskeletal rearrangement and cell body polarization (Figure 2.5B). This experiment demonstrated that

we can use NVOC-SDF1α to control chemokine receptor activation with high spatiotemporal specificity.

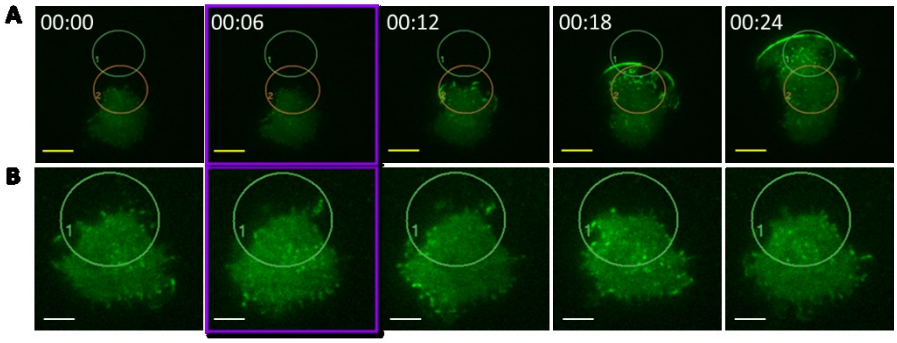

Figure 2.5 NVOC-SDF1α can be used in combination with a video-microscopy platform to control chemotactic signal transduction with high spatiotemporal resolution. Jurkat T-cells transduced with Wave2-GFP were adhered to glass surfaces coated with (A) NVOC-SDF1α and fibronectin or (B) fibronectin alone. Circles indicate regions of focused UV irradiation. Purple frames indicate photoactivation. Image acquisition was done using a TIRF microscope objective. Yellow scale bar = 5μm and white scale bar = 2.5 μm. Time is shown in A as MM:SS and correspond to the frames in the montage in B, as well.

Having shown that NVOC-SDF1α can be used to activate chemokine receptor signaling with high spatial and temporal resolution in a live cell microscopy experiment, we wanted to apply our system to dissect the complex signaling circuits involved in a chemotactic response. One of the major signaling pathways activated downstream of chemokine receptor stimulation is the PI3K pathway. It is appreciated that PI3Kγ, the sole member of the class IB PI3K family, is involved in chemotactic signaling[86,87].

PI3Kγ is a membrane lipid kinase consisting of a catalytic subunit p110γ and one of two regulatory subunits p101 and p87. Chemokine induced activation of PI3Kγ is dependent upon plasma membrane recruitment of the catalytic/regulatory subunit complex. At the plasma membrane, G proteins through a mechanism not yet fully understood allosterically activate the kinase's phosphatidylinositol phosphorylation activity[88]. The plasma membrane recruitment of the p110γ/p101 complex is mediated via direct binding to the Gβγ G-protein. Accordingly, both p101and p110γ subunits contain Gβγ binding domains. It was not until recently, however that the mechanism of p110γ/p87 membrane recruitment was discovered to be different from that of p110γ/p101. Indeed, it was shown that upon chemokine receptor activation, Ras-GTP is activated and via direct binding to p110γ recruits the p110γ/p87 complex to the membrane[89]. All this characterization was done biochemically. The temporal and spatial aspects of these two distinct mechanisms of activating PI3Kγ activity remain uncharacterized. Our photoactivation system is uniquely suited for this purpose.

To investigate the spatial and temporal dynamics of p101 and p87 membrane recruitment, we transduced constructs encoding GFP fused N-terminally to either p101 or p87 into Jurkat T-cells, and performed photoactivation similar to the experiment described in Figure 2.5. Upon photoactivation, we observed a rapid, local and sustained accumulation of p101 at the plasma membrane. Remarkably, this accumulation was restricted to within the region of UV –irradiation. GFP-p87 also accumulated at the region of irradiation but in a distinct spatiotemporal pattern. Upon photoactivation, p87 was recruited to the plasma membrane transiently. As a

control, we also performed photoactivation with Jurkat cells expressing GFP-p85α, which is a regulatory subunit of class IA PI3K. As class IA PI3Ks are not activated downstream of chemokine receptor activation, we expected and indeed observed no membrane recruitment of p85 upon photoactivation (Figure 2.6). We also performed photoactivation in the presence of a CXCR4 specific inhibitor, AMD3100, to confirm that the observed membrane recruitment of p101 and p87 was as a result of CXCR4 receptor activation (Figure 2.7 and Figure 2.8).

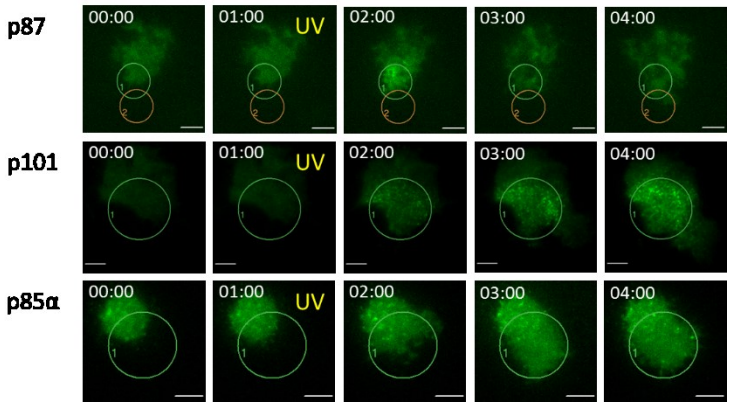

Figure 2.6 Photoactivation of Jurkat T-cells specifically induces local clustering and membrane recruitment of the regulatory subunits of PI3Ky. Jurkat T-cells transduced with N-terminal GFP-tagged p101, p87 and P55 alpha were photo activated on glass surfaces coated with NVOC-SDF1alpha and fibronectin. Membrane dynamics were imaged using a TIRF microscope.

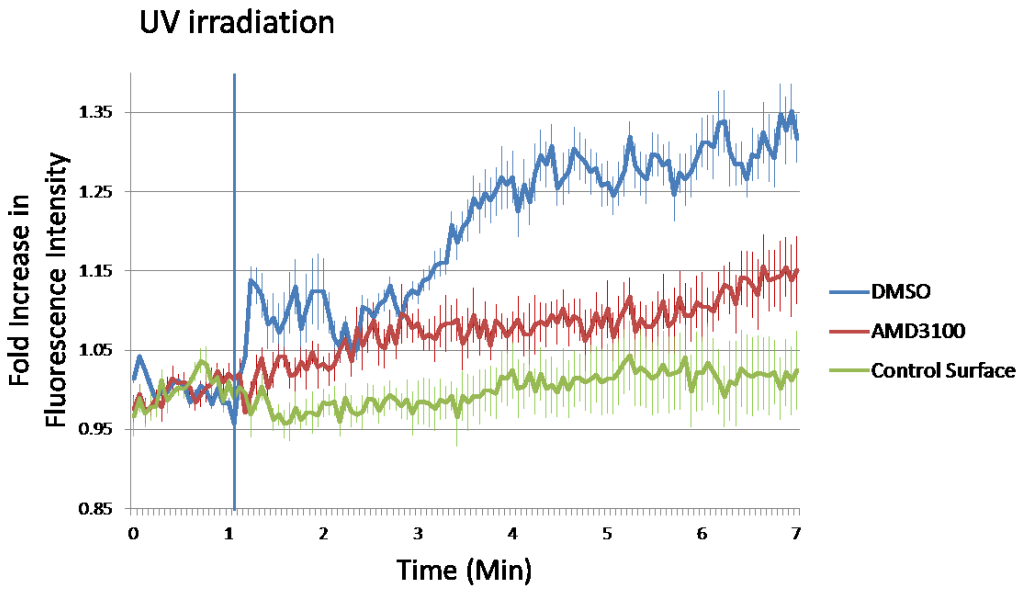

Figure 2.7 Plasma membrane recruitment of p101 upon photoactivation requires CXCR4 activation. The line graph shows quantification of the clustering in the region of UV-irradiation as function of time. An increase in mean fluorescence intensity indicates clustering or recruitment of GFP-p101 to the plasma membrane in the irradiated region. Jurkat cells expressing GFP-p101 were photo-activated on glass surface coated with NVOC-SDF1α in the presence of vehicle control DMSO (blue line) or the CXCR4 inhibitor AMD3100 (red line). Photoactivation was also performed on glass surfaces coated with fibronectin alone (green line) to control for UV-damage-induced signaling. Photoactivation is indicated by the blue vertical line.

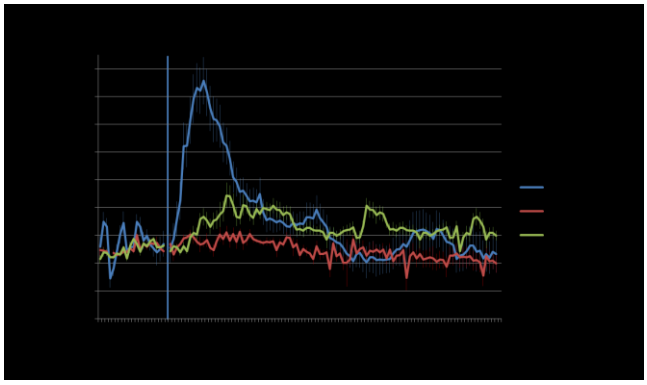

Figure 2.8 Plasma membrane recruitment of p87 upon photoactivation requires CXCR4 activation. The line graph shows quantification of the clustering in the region of UV-irradiation as function of time. An increase in mean fluorescence intensity indicates clustering or recruitment of GFP-p87 to the plasma membrane in the irradiated region. Jurkat cells expressing GFP-p87 were photo-activated on glass surface coated with NVOC-SDF1α in the presence of vehicle control DMSO (blue line) or the CXCR4 inhibitor AMD3100 (red line). Photoactivation was also performed on glass surfaces coated with fibronectin alone (green line) to control for UV-damage-induced signaling. Photoactivation is indicated by the blue vertical line.

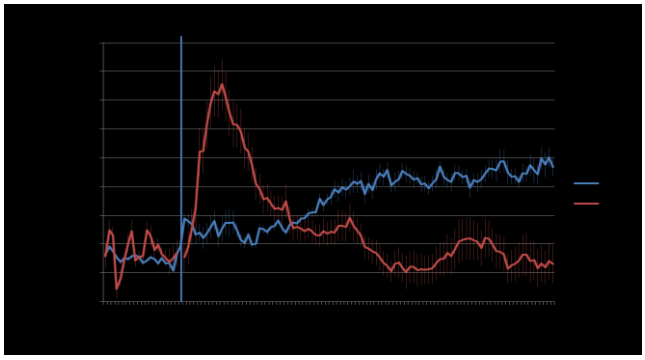

.

Figure 2.9 p101 and p87 have different membrane recruitment profiles upon photoactivation.

2.3 DISCUSSION:

We have developed a photoactivatable chemokine SDF1α. We demonstrated that this reagent could be used to control activation of the chemokine receptor CXCR4 with high spatial and temporal specificity. With the observations of the membrane recruitment dynamics of p101 and p87 afforded by our photoactivation platform, we have also showed for the first time, the difference in the spatial and temporal aspects of signal transduction between the two regulatory subunits of PI3Kγ. There are outstanding questions to be addressed regarding the difference in p101 and p87 membrane recruitment. From our correlation analysis (Figure 2.9), it seems that p101 and p87 were recruited to the membrane at approximately the same time suggesting that there were parallel pathways at work. It is known that Gβγ directly binds and recruits p101. Not much however is known regarding the mechanism of p87 membrane recruitment. Indeed, membrane bound Ras has been implicated in p87 recruitment but the intervening signaling pathway upstream of Ras activation and downstream of CXCR4 stimulation is not known. As p87 recruitment was observed within seconds after photoactivation, the upstream signaling pathway is likely to involve signaling components near or at the plasma membrane. One promising candidate is RasGRP1 which is a prominent RAS-GEF involved lymphocyte signaling. In other signaling contexts, upon cellular activation, RasGRP1 is recruited to the plasma membrane via a diacylglycerol (DAG) dependent mechanism[90]. Upon CXCR4 activation however, it was shown that RasGRP1 was recruited to the plasma membrane in a DAG-independent manner via direct binding to the Gαi G-protein[91]. DAG-independent recruitment of

RasGRP1 is therefore a fast reaction whose dynamics could support the rapid recruitment of p87. Assessing GFP-p87 membrane recruitment in a RasGRP1 shRNA knockdown background in a photoactivation experiment would directly address the role RasGRP1 in p87 membrane dynamics. Additionally, simultaneous imaging of RasGRP1 and p87 tagged with different fluorescent proteins would provide key correlative observations. Other known RasGEFs such as Grb2/SOS must also be considered.

The broader question regarding the difference in membrane dynamics of p87 and p101 rests on the functional implication of these two potentially parallel pathways in PI3Kγ activation. In mast cells and macrophages, p87 was shown to control degranulation and ROS-production, whereas p101 was shown to mediate other cellular effects[89]. In neutrophil chemotaxis, it was revealed that PI3K signaling, upon cellular activation, was propagated by two functionally distinct signaling circuits. One regulated Rac-driven membrane protrusion while the other via unknown mechanism set up a cytoskeletal polarity axis within the cell[92]. These observations, taken together with the difference in the membrane recruitment dynamics of p87 and p101 that we observed, suggest a hypothesis where the two regulatory subunits might play distinct roles in regulating cytoskeletal dynamics. p101's sustained membrane localization, for instance, might serve as the signal setting up the anterior-posterior axis which is sustained throughout the duration of a migratory response. By contrast, p87's transient and burst-like membrane recruitment might serve as the activating signal that regulates Rac-dependent membrane protrusion which in itself is a highly dynamic process.

As discussed previously in chapter 2 and the beginning of this chapter, a long standing interest in the field of chemotaxis focuses on the spatial and temporal organization of the signaling events following chemokine receptor activation. Our goal in developing a photoactivatable chemokine was to provide a tool that allows for precise perturbations and quantitative observations. We hope to construct a better spatiotemporal model of polarized signaling events that culminate in the establishment of migratory cell polarity and directional movement. The p101 and p87 membrane dynamics that we have observed are compelling examples of the kind quantitative and precise observations that a light-gated technology, in this case a photoactivatable chemokine, can provide.

2.4 MATERIALS and METHODOLOGY:

General methods and Reagents. Recombinant SDF1α was purchased from Peprotech. Human Fibronectin and AMD31000 were purchased from Sigma Aldrich. PCR primers and templates were purchased from Integrated DNA Technologies. Unless otherwise indicated, all expression plasmids were purchased from Addgene. Fmoc-protected amino acids were obtained from Merck Millipore, and all other chemicals used in solid phase peptide synthesis were purchased from Sigma Aldrich. Synthesis grade organic solvents were from Fisher Scientific. Peptide purification and small molecule purification were carried out using an HPLC system (Waters) outfitted with a C18 reversed phase column (VYDAC.) Mass spectrometry data was obtained by LC-MS (Agilent Technologies) at the Memorial Sloan Kettering Cancer Center Mass Spectrometry Core Facility.

Solid Phase Peptide Synthesis of Caged SDF1α. Synthesis of the NVOC-SDF1α was carried out using standard FMOC-solid phase peptide synthesis. PEGylated rink resin (NovaPEG Rink Amide Resin. Novabiochem. Catalog no:855047) was used for chain extension to aid with solubility and avoid chain collapse. SPPS reactions were carried out in a custom-made glass peptide synthesis vessel (Adams & Chittenden). A constant stream of nitrogen was used to provide gentle agitation. Amino acid coupling was performed using HBTU as the carboxylic acid activating agent and DIPEA as the organic base in DMF solvent. For each coupling reaction: 3 eq of FMOC-AA-OH, 2.9 eq of HBTU and 3 eq of DIPEA were used. Coupling time was one hour at room temperature. Deprotection of FMOC was performed with 20% Piperidine/DMF for 20 minutes. The peptide was then purified by HPLC using a water/acetonitrile gradient

Folding and purification of caged SDF1. HPLC purified and lyophilized NVOC-SDF1α was dissolved at 0.2 mg/mL in 1 M guanidine, 150 mM NaCl, 3 mM EDTA, 0.3 mM reduced glutathione and 3 mM oxidized glutathione at pH 8.6. Folding was done at room temperature with gentle agitation for 2 hours. Folding solution was allowed to pass through a desalting column (Disposable PD-10 Desalting Column. GE LifeSciences. Catalog no: 17-0851-01) that has been buffer exchanged with PBS. Refolded NVOC-SDF1α was eluted with PBS and stored at 4^{o}C.

FACS-based fluorescent calcium flux assay. Primary T-cells were loaded with Flou-4AM calcium indicator (Life Technologies, catalog no: F-14201) for 30 minutes. Cells were then washed and re-suspended in 37^{o}C complete

RPMI supplemented with probenecid acid to stop dye leakage. Dye loaded T-cells were transferred to a FACS tube and immediately put on flow cytometer for data collection. During data acquisition, SDF1α dissolved in warm RPMI was added to the tube to a final concentration of 100ng/mL.

Chemotaxis transwell assay. Transwell assays were carried out using a 96 well transwell apparatus outfitted with a 5 μM filter (NeuroProbe Chemo Tx# 101-5). T-cells were suspended in complete RPMI supplemented with 25 mM HEPES and 10 mg/mL BSA at 1.5 million cells per mL. 45 uL aliquots of cell suspension were used atop each well. Chemokine was dissolved in the same chemotactic buffer at 4 different concentrations: 1μg/mL, 100 ng/mL, 10 ng/mL and 1 ng/mL. Cells were allowed to migrate in tissue culture hood (37^{o}C and 5% CO_2) for 1 hour. The in between filter was then removed and cells that had migrated to the bottom wells were collected and transferred to FACS tube containing 200 μL FACS cell counting buffer (PBS with 5% FBS,1 mM EDTA and 0.1% sodium azide) with flow cytometer reference beads (PeakFlow , Invitrogen Catalog no: P14825) at 20 000 beads per mL. The empty wells were washed once with another 200 μL FACS cell counting buffer. Cell counting was performed by gating on a fixed number of reference beads.

Expression vector construction. Coding sequences for mouse Wave2 was cloned into pMSCV vector upstream of eGFP. Coding sequences of mouse p85α, p101 and p87 were cloned into a shuttled vector derived from pTOPO (Intvitrogen) downstream of GFP (NT-GFP-TOPO). Fragments encoding the fusion protein were then cut out and ligated into pMSCV.

Cell Culture and Retroviral Transduction. Jurkat E 6.1 T-cells (American Type Culture Collection) were maintained in complete RPMI supplemented with 10% fetal bovine serum (FBS) and antibiotics. Transduction was carried using an amphotrophic retroviral system with pMSCV expression plasmids and pCMV-Gag-Pol packaging plasmid. Pheonix A cells at about 90% confluency were transfected with the aforementioned retroviral expression and packaging plasmids by calcium phosphate method. Viral supernatants were collected after 48 hr at 37^0C and added to 1 million exponentially dividing Jurkat cells (which were subcultured two days prior at 200 000 cells per mL) in a 6-well tissue culture plates. Mixtures were subsequently centrifuged at 1000 g in the presence of polybrene (4 μg/mL) at 35^0C for 2 hr and allowed to incubate overnight at 37^0C. Cells were then expanded in fresh medium.

Photoactivation and TIRF video microscopy experiment. Glass surfaces for photoactivation were prepared from eight-well chamber slides (Nunc). Chamber slides were washed in Hellmanex III solution (Hellma Analytics, Catalog no: 9-307-010-507), rinsed thoroughly and stored in double distilled water. The day before imaging, 150 μl mixture of fibronectin (20 μg/mL) and chemokine (100 ng/mL) was added to each well and incubated overnight at 4^0C. Just before imaging, the coated glass slides were allowed to warm up to room temperature and washed three times with PBS. Jurkat cells were allowed to adhere to coated chamber slides for 10 mins before data collection in cRPMI. For pharmacological treatment, inhibitor (AMD3100 at 5 μM) was added after imaging acquisition had been done on at least 3 cells. Live imaging experiments were carried out using an inverted fluorescence

video microscope fitted with a 150X objective with a numerical aperture of 1.45 (Olympus). Laser at 488 nm (Melles Griot) was used for epifluorescence imaging of GFP. A Mosaic digital diaphragm apparatus (Photonic Instruments) attached to a mercury (HBO) lamp (Olympus) was used for photoactivation. Time-lapse recordings were made with Slidebook software (Intelligent Imaging Innovations). Images were acquired every 3 seconds. Cells were activated with a UV exposure of 3 seconds.

P101 and P87 recruitment quantification. GFP-p101 and GFP-p87 membrane recruitment were quantified by determining the mean fluorescence intensity inside of the irradiated regions, after background correction, as a function of time. Image analysis was performed using Slidebook, Microsoft Excel, and GraphPad Prism.

CHAPTER 3: A generalizable platform for the photoactivation of cell surface receptors

3.1 INTRODUCTION:

3.1.1 The biological significance of cell polarity.

Cell polarity is the asymmetrical organization of cellular structures and components within the cell. It is a fundamental process that allows cells across the phyla to effectively carry out their biological purposes. Cell polarity is most evident in cells that have specialized functions. Neurons, for example, exhibit dramatic polarization of the cell body. During development, neural progenitors transform from isotropic spheres into a complex and polarized architecture containing several shorter dendrites at one end and a long axon at the other[93]. The extension of the axons is driven by highly polarized cellular structures called growth cones. The growth cone functions by sensing environmental cues in the form of soluble ligands and translates those signals into cytoskeletal dynamics to support directional growth of the axon[94]. The compartmentalization of the neuronal cell body into molecularly and functionally distinct segments, in other words its polarity, is critical to a neuron's development and the functionality of neuronal networks. Similar to the concept of growth cones driving axon extension, during vasculogenesis, certain endothelial cells lining blood vessels, via unknown mechanism, assume the role of guiding "tip" cells, which upon detecting extracellular angiogenic cues polarize their cell body and migrate outward[95]. The polarization of blood vessel endothelial cells into tip cells is the critical first

step in the “sprouting” of new blood vessels from existing ones in response to extracellular signals.

Migratory cells represent another dramatic example of cell polarity. As has been discussed in greater detail in chapter 2, the breaking of symmetry and polarization of the cell body into a migratory form is the critical first step to ensure productive directional migration of leukocytes in response to extracellular stimuli. Another form of cell polarity that is critical to the function of a T-cell occurs during cell-to-cell contact between an antigen specific T-cell and an antigen-presenting target cell. T-cells function in part by making direct contact with target cells after which the T-cells would, depending on context, directionally secret of cytotoxic factors or regulatory cytokines and exert cell-mediated immunity. Stimulation of the TCR by a target cell induces dramatic reorganization of the T-cell’s body whereby a special structure is formed at the contact interface known as the immunological synapse[96]. It is towards the immunological synapse that an activated T-cell polarizes critical organelles and structures such as the microtubule organizing center (MTOC) and secretory machinery. Such cellular polarization facilitates directional secretion which is central to the function of a T-cell[97]. It is worth noting that very similar forms of cell polarity exist in other cell-cell contact contexts such as virological synapses, which form between virally infected T-cells, and NK cells synapses, which form between NK cells and their target cells.

Given that cell polarity is crucial for many of the complex biological processes we associate with eukaryotic cells, it is unsurprising that cell polarity and the dys-regulation of it significantly to disease conditions. The

pathology of arthritic joints, for example, is characterized by the recruitment and infiltration of inflammatory leukocytes to the affected joints[98] . Therapies aimed at reducing the migration of inflammatory leukocytes to the arthritic joints are currently in the clinical trials. In tumor biology, the loss of epithelial cell polarity initiates the epithelial-mesenchymal transitions (EMTs) that turn healthy polarized epithelial cells into mesenchymal cells that are resistant to apoptosis and exhibit increased migratory capabilities[99]. The dys-regulation of epithelial cell polarity ultimately leads to invasive oncogenic growth and metastasis [99,100].

3.1.2 The acquisition and maintenance of cell polarity are driven by cell surface receptors and their cognate extracellular ligands.

The segregation of cellular and signaling components into spatially distinct regions in the cell during polarized signal transduction is initiated at the plasma membrane. Cell surface receptors, activated by the binding of extracellular ligands, trigger cascades of signaling events that propagate down throughout the cell cytoplasm. The integration of these signaling events in space and time sets up a polarity axis inside the cell and facilitates subsequent cellular processes. In the case of the neuronal growth cone, cell surface receptors detect molecular guidance cues in the form of soluble secreted proteins. Upon activation, these cell surface receptors initiate signaling cascades that culminate in the reorganization of the cytoskeleton to move or turn the growth cone in the direction from which the extracellular cues originate[94]. In the case of chemotaxis in lymphocytes, a similar polarized signal transduction program is observed. Chemoattractants, upon

binding to chemokine receptors, trigger signal transduction programs to polarize the cell body and propel the cell towards the source of the chemoattractants[75]. Similar processes of polarized signal transduction from cell surface receptors underlie other forms of cell polarity such as tip cells' polarization during vasculogenesis and the formation of the immunological synapse upon TCR activation.

While the individual proteins and pathways that get activated to initiate and maintain cell polarity in different contexts have mostly been identified and characterized, much less is understood regarding how these circuits are integrated temporally and spatially throughout the cell. Traditional experimental tools such as genetic knockdown and small molecule inhibitors are great at identifying key players in polarized signal transduction. Such techniques however lack the spatial and temporal control to provide quantitative measurements about polarized signaling dynamics. High resolution imaging techniques coupled with the use of fluorescent proteins and antibody staining, while useful in providing snapshots of the spatial organization of circuits downstream of cell surface receptor activation during polarized signaling, cannot be used to perturb and establish cause and effects relationships between signaling events. Deciphering the complex molecular choreography involved in cell surface receptor polarized signaling requires tools that combine the monitoring and perturbation of signaling pathways with high spatiotemporal resolution.

3.1.3 Photo-caged extracellular ligands are effective tools to perturb polarized signaling from cell surface receptors with high spatiotemporal resolution.

In recent years, a number of optogenetic systems have been engineered for the controlled activation of cell surface receptors. As summarized in chapter 1, light sensitive rhodopsin-GPCR chimeras (optoXRs) have emerged as useful tools in the studies of neuronal transmission and cellular chemotaxis[45,46]. In addition, photosensitive proteins derived from plants have been used to enable light-controlled stimulation of cell surface receptors and/or their downstream signaling components. Although these methods provide exquisite control over where and when signaling molecules are activated, restraining the rapid diffusion of these molecules away from the illuminated region after stimulation has proven to be a formidable technical challenge. This has limited the applicability of optogenetics in studies that require both sustained and subcellular stimulation.

As previously discussed, photo-caged ligands immobilized on solid surfaces provide both spatial and temporal control of the activating signal. Chapter 2 described one such photocaged ligand. The caged ligand developed there was the chemokine SDF1α. While the critical role of the chemokine's N-terminal lysine residue and the relatively small size of the protein lent themselves easily to a caging strategy and straightforward chemical synthesis, the majority of protein ligands present major photocaging design hurdles. For example, protein ligands can be large in size which limits synthetic access. Furthermore, ligands can have complicated mechanisms

of activating their receptors where the agonist activity is not localized to any particular residues but is rather controlled by structural domains or motifs. In such cases, effective photocaging strategies would either be too cumbersome or technically unfeasible. It would be of great interest therefore if there were a universal ligand platform that allows for the activation of multiple cell surface receptors via the use of one single caged ligand. Such a system would sidestep the challenge of having to design and engineer an individual photocaged ligand for every receptor.

3.1.4 The design of a universal caged ligand platform relies on the modularity of receptor proteins.

Many cell surface receptors, including receptor tyrosine kinases (RTKs) and cytokine receptors, are type I transmembrane proteins that function via ligand-induced dimerization. In this regime, the act of ligand binding brings together two receptor chains such that their cytoplasmic tails, which either contain tyrosine kinase domains or interact with non-receptor tyrosine kinases, become close enough to promote trans-autophosphorylation and downstream signaling. The extracellular domains of the receptor typically mediate ligand binding, while the intracellular tails control signal transduction. This architectural modularity has allowed for the design of functional chimeric receptors that contain the cytoplasmic tail of one receptor fused to the extracellular domain of another. In principle a ligand for one receptor could be used to activate signaling associated with another receptor via the use of chimeras. Hence, if one could develop an effective caged ligand for a “parent” receptor-ligand pair, it could, in principle, be used to

elicit signaling from a wide range of chimeric receptors containing the extracellular domain of the parent receptor and the intracellular signal transduction domains of other receptors of interest.

Erythropoietin receptor (EpoR) and its ligands are uniquely suited as the parent receptor-ligand pair for the development of the universal caged ligand-chimeric receptor platform. EpoR is a well characterized prototypical type 1 transmembrane cytokine receptor. EpoR and its cognate ligand Epo are key regulators of erythropoiesis – the differentiation of red blood cells from hematopoietic progenitors. The binding of the166 AA Epo protein, to EpoR, which exists as a preformed dimer, induces conformation changes that lead to receptor activation[101,102]. Importantly, EpoR has been successfully used to create functional chimeric receptors containing the extracellular domain of EpoR fused to the transmembrane and intracellular domains of other receptors[103,104]. EpoR-chimeras are therefore likely to be functional receptors. From the photo-caged ligand perspective, the large size of the Epo protein renders the design of a caged ligand difficult. Interestingly however, a small 20 amino acid long peptide called EMP1 was discovered to be a potent activator of EpoR with nanomolar affinity[105,106]. Furthermore, a structural study of EMP1 has localized the agonist activity of the ligand to a tyrosine residue near the N-terminus (tyrosine 4)[105]. It follows then that a caged ligand for EpoR could be synthesized by installing a UV-cleavable group onto EMP1 Tyr4.

We hypothesized that the use of chimeric receptors containing the extracellular domain of EPOR and the intracellular domains of receptors of

interest, in combination with a photo-caged EMP1 ligand, would constitute a universal platform to control cell surface receptor activation via light-induced receptor dimerization. We envisioned the photo-caged EMP1 ligand platform to be a tool that allows for sustained, local stimulation of cell surface receptors. By adhering cells expressing chimeric receptors of interest on top of glass surface pre-coated with caged EMP1 ligand, focused light pulses could be used to locally de-cage and deliver an activating signal to the cell. As the decaged ligands would remain bound to the glass surface outside of the cell, a sustained and spatially constrained activating signal could be achieved (Figure 3.1)

The rest of this chapter will discuss the synthesis of a caged analog of the EMP1 ligand. It also details experiments validating the utility of this photosensitive ligand to activate a range of cell surface receptors in a light dependent manner. Finally, it describes efforts to demonstrate that this universal platform can be used in live cell videomicroscopy experiments to activate cell surface receptors in a spatiotemporally precise manner. The strategy to synthesize a caged EMP1 ligand focuses on Tyrosine 4. Mutagenesis studies have shown that replacement of this amino acid with non-polar amino acids such as Phenylalanine or Alanine reduced the agonist activity of the ligand by 2 orders of magnitude[105]. We reasoned that by installing a UV-cleavable NVOC group on the side chain of Tyr4, the agonist activity of EMP1 would affectively be photo-caged. . The strategy to synthesize a caged EMP1 ligand focuses on Tyrosine 4.

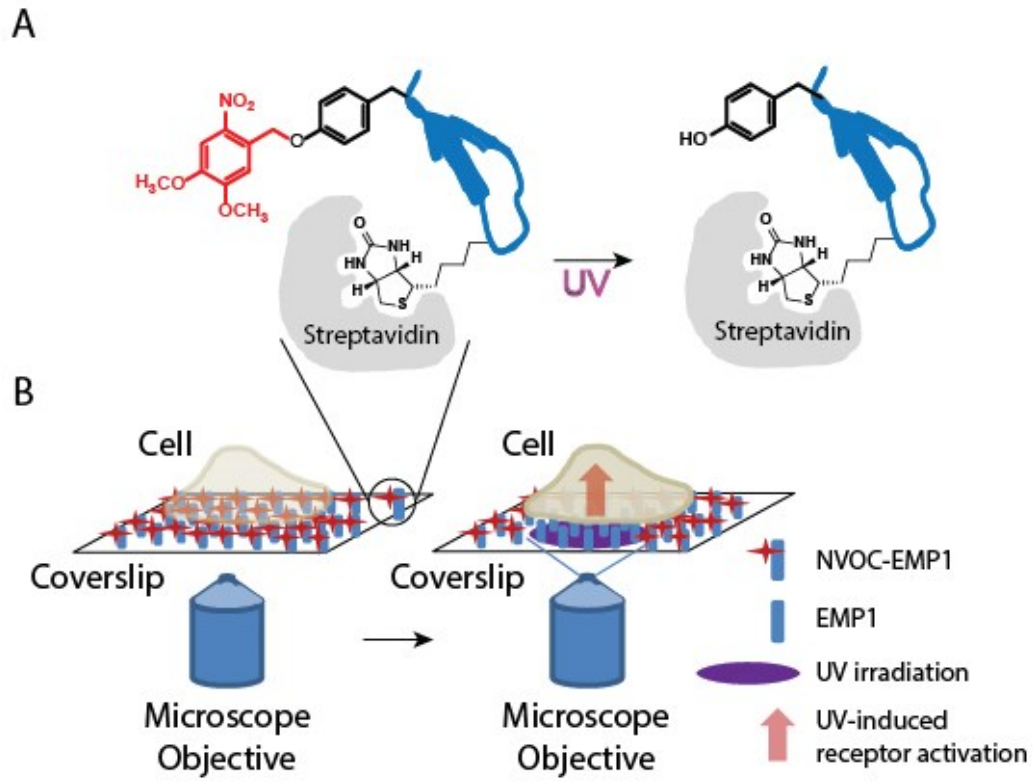

Figure 3.1 A generalizable platform for the UV dependent activation of cell surface receptors. (A) EMP1 is photocaged on Tyr4 with a UV-sensitive caging group and contains a C-terminal biotin tag. It cannot dimerize EpoR until UV irradiation removes the caging moiety (in red). (B) Schematic of a photoactivation videomicroscopy experiment. Caged EMP1 ligand is immobilized via a streptavidin-biotin linkage on a glass coverslip. After cells are attached to the glass, focused UV light is used to decage the surface beneath an individual cell. Subsequent receptor activation and signal transduction can be observed in real time using fluorescent signaling probes.

.3.2 RESULTS:

3.2.1 Synthesis of a caged EMP1 ligand.

The strategy to synthesize a caged EMP1 ligand focuses on Tyrosine 4. Mutagenesis studies have shown that replacement of this amino acid with non-polar amino acids such as Phenylalanine or Alanine reduced the agonist activity of the ligand by 2 orders of magnitude[105]. We reasoned that by installing a UV-cleavable NVOC group on the side chain of Tyr4, the agonist activity of EMP1 would affectively be photo-caged. We hypothesized that bulky NVOC group would interfere with critical interactions between the ligand and EPOR otherwise facilitated by Tyr4. The synthesis of the photo-caged EMP1 hereafter referred to as NVOC-EMP1, was carried out via FMOC-solid phase peptide synthesis. The full sequence of NVOC-EMP1 includes a 23 amino acid polypeptide of the following composition: GGTY(NVOC) SCHF GPLT WVCK PQGG SSK(Biotin). We extended the original EMP1 peptide by adding three additional amino acids SSK at the C-terminus to facilitate the installation of a biotin molecule. A biotinylated EMP1 is important for glass surface immobilization via the use of streptavidin. The synthesis of EMP1 is outline in Scheme 3.2. The complete secondary structure of EMP1 ligand features a disulfide bond formed between the two cysteine residues. Since there are only two cysteine residues present in the peptide, disulfide bond formation was straightforward. After HPLC purification and lyophilization, the peptide was dissolved in 10% DMSO/phosphate buffered saline (PBS) and exposed to air overnight to induce disulfide bond formation. To confirm that upon UV irradiation the NVOC undergoes a clean photolysis from the EMP1 peptide, we subjected the molecule to irradiation using a hand-held UV lamp and analyzed the product by HPLC and mass spectrometry. As expected, UV-irradiation of this

peptide removed the NVOC moiety, yielding the unmodified EMP1 (Figure 3.3).

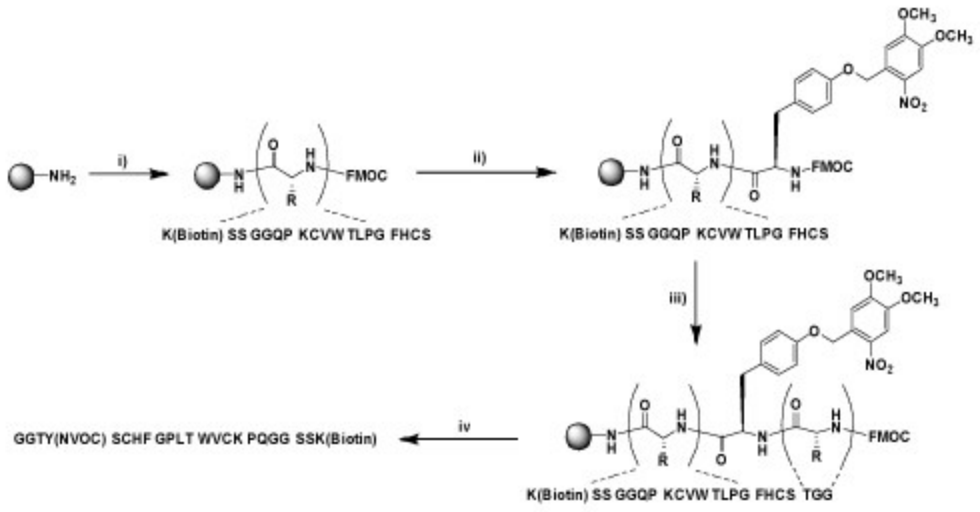

Figure 3.2 Synthesis of NVOC-EMP1. i) Rink resin, Fmoc-AA-OH, HBTU, DIPEA in DMF; FMOC-Tyr(NVOC)-OH, HBTU, DIPEA in DMF; Fmoc-AA-OH, HBTU, DIPEA in DMF; 82.5% TFA, 5% water, 5% phenol, 5% thioanisole, 2.5% 1,2-ethanedithiol. Rink resin, Fmoc-AA-OH, HBTU, DIPEA in DMF; FMOC-Tyr(NVOC)-OH, HBTU, DIPEA in DMF; Fmoc-AA-OH, HBTU, DIPEA in DMF; 82.5% TFA, 5% water, 5% phenol, 5% thioanisole, 2.5% 1,2-ethanedithiol. Rink resin, Fmoc-AA-OH, HBTU, DIPEA in DMF; FMOC-Tyr(NVOC)-OH, HBTU, DIPEA in DMF; Fmoc-AA-OH, HBTU,

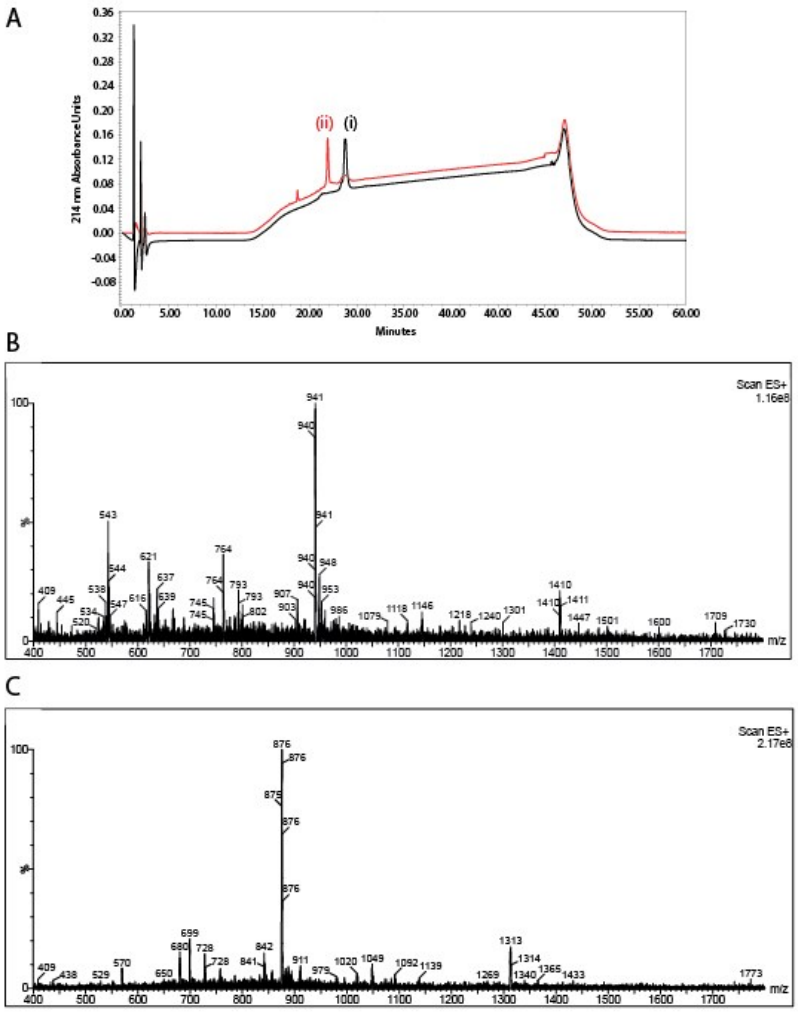

Figure 3.3 (A) Reversed phase elution profiles of NVOC-EMP1 (Black) and NVOC-EMP1 irradiated with a handheld UV lamp for 15 minutes (Red). UV irradiation removes the NVOC moiety from the phenolic oxygen of Tyr4 and shifts the elution profile of the peptide. (B) ESI mass spectrometry analysis of purified absorption peak **(i)**. The predicted molecular weight of NVOC-EMP1 ($C_{125}H_{180}N_{32}O_{37}S_3$) is 2817.25. Found $[M+H]^{3+}$: 940. (C) ESI mass spectrometry analysis of purified absorption peak **(ii)**.

3.2.2 NVOC-EMP1 is a photoactivatable ligand for EpoR

Before using NVOC-EMP1 as a ligand to activate chimeric receptors, we wanted to assess the capacity of NVOC-EMP1 to function as a caged ligand for its cognate receptor EpoR. We performed a bioassay using the TF1 cell line. TF1 cells were established from a patient with erythroleukemia. These cells express EpoR at a high level and stimulation with Epo induces their differentiation along the erythroid lineage[107]. Treatment of TF1 cells with Epo induces robust phosphorylation of the transcription factor Stat5a (Figure 3.4). When used to stimulated TF1 cells in solution, NVOC-EMP1 failed to induce this response, suggesting that the caging group disrupts productive EpoR binding. After UV irradiation, however, the peptide elicited strong Stat5a phosphorylation (Figure 3.5). Hence, NVOC modification of EMP1 on Tyr4 effectively photocages the activity of this molecule. Treatment of TF1 cells with Epo induces robust phosphorylation of the transcription factor Stat5a (Figure 3.4). When used to stimulated TF1 cells in solution, NVOC-EMP1 failed to induce this response, suggesting that the caging group disrupts productive EpoR binding. After UV irradiation, however, the peptide elicited strong Stat5a phosphorylation (Figure 3.5). Hence, NVOC modification of EMP1 on Tyr4 effectively photocages the activity of this molecule. Treatment of TF1 cells with Epo induces robust phosphorylation of the transcription factor Stat5a.

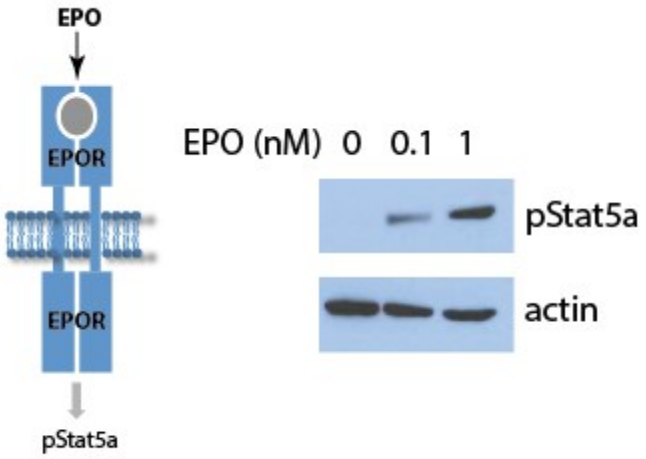

Figure 3.4 EPO stimulation of TF1 cells induces phosphorylation of Stat5a. Serum and cytokine starved TF1 cells were stimulated with EPO at indicated concentrations for 10 minutes. Cells were immediately lysed and phosphor-Stat5a levels were assessed by immunoblot. Actin served as a loading control

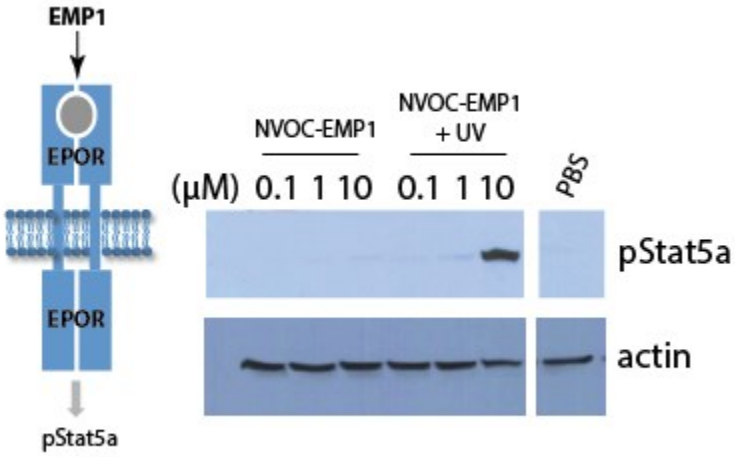

Figure 3.5 TF1 cells were treated with the indicated concentrations of NVOC-EMP1 that had either been irradiated with UV light or left untreated. EpoR signaling was assessed by immunoblot for phosphorylated Stat5a.

3.2.3 NVOC-EMP1 can act as a photoactivatable ligand for multiple receptors.

Having proved that NVOC-EMP1 is an effective ligand to control the activation of EpoR in a UV-dependent manner, the next step was to prove that we could use NVOC-EMP1 to access other signaling systems using EpoR chimeras. Our initial efforts focused on two receptor tyrosine kinases, Epidermal Growth Factor Receptor (EGFR) and Tropomyosin receptor kinase A (TrkA). EGFR regulates growth and homeostasis in multiple epithelial cell types and is often dysregulated in cancer[108]. Upon binding to its cognate ligand EGF, EGFR undergoes a series of conformation changes resulting in the phosphorylation of tyrosine residues in the receptor's cytoplasmic domain which can be detected biochemically (Figure 3.6). Due to the robustness of the tyrosine phosphorylation events as readouts for receptor activation upon ligand binding, we chose EGFR as the first proof of principle test receptor for the NVOC-EMP1-EpoR chimeric platform.

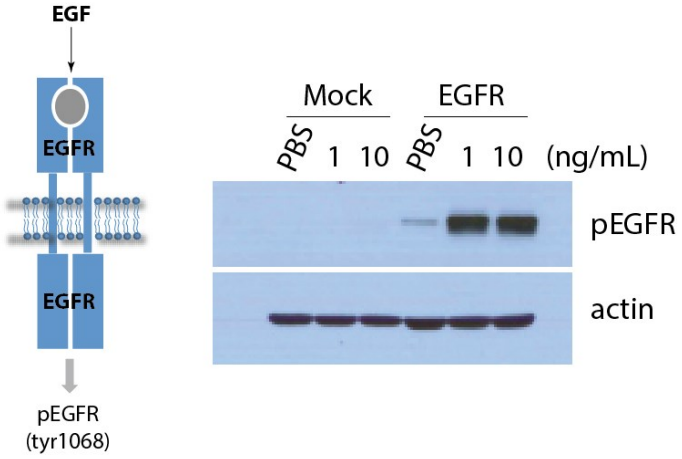

Figure 3.6 NIH3T3 cells were transfected to express full length EGFR and stimulated with EGF at the indicated concentrations.

To demonstrate that NVOC-EMP1 can drive EGFR dependent signals, we prepared chimeric constructs containing the extracellular domain of EpoR and the cytoplasmic domains of EGFR. NIH-3T3 cells expressing the EpoR-EGFR chimera were unresponsive when treated with NVOC-EMP1, as evidenced by the absence of ligand-induced receptor phosphorylation (Figure 3.7). Treatment of these cells with the UV-irradiated peptide, however, elicited robust signaling, validating both the functionality of the EpoR-EGFR construct and the efficacy of NVOC-EMP1 as a caged ligand.

We next looked at TrkA. TrkA is a receptor tyrosine kinase that is highly expressed in the nervous system. Upon binding to its cognate ligand, nerve growth factor (NGF), TrkA undergoes dimerization followed by autophosphorylation and a signaling cascade[109]. NGF was the first identified neurotrophin and has a wide range of functions in neuronal development. TrkA-NGF signaling for example regulates neuron survival. *In vitro* treatment of dorsal root ganglion (DRG) with NGF strongly promotes nerve fiber elongation and sprouting. In the context of neuronal cell polarity, upon detecting NGF in the extracellular environment, TrkA initiates polarized signaling cascades that culminate in the turning of axon growth cones towards the source of NGF[110]. Since the purpose of the development of the NVOC-EMP1 is to aid in the study of receptor surface receptors that regulate cell polarity, TrkA was an interesting receptor.

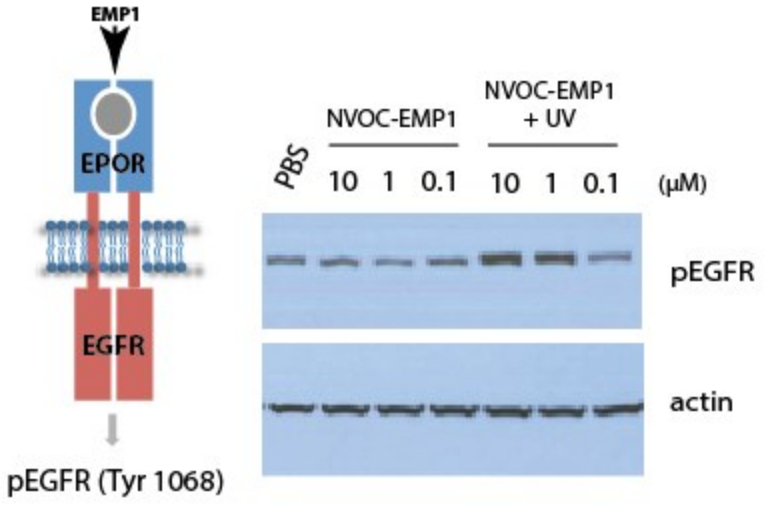

Figure 3.7 NIH-3T3 cells expressing EpoR-EGFR were treated with the indicated concentrations of NVOC-EMP1 that had either been irradiated with UV light or left untreated. EGFR signaling was assessed by immunoblot for Tyr 1068 phosphorylation.

To demonstrate that NVOC-EMP1 can be used to activate TrkA dependent signaling in a UV dependent manner, we created chimeric constructs containing the extracellular domain of EpoR and the cytoplasmic domains of TrkATrkA activates the mitogen-activated protein kinases (MAPK) pathway[109]. Indeed, when expressed in NIH3T3 cells, full length TrKA receptors were able to rapidly and robustly induce the phosphorylation of Erk1/2 (Figure 3.8). We therefore used the phosphorylation states of Erk1/2 as the biochemical readouts for TrkA dependent signaling. By assessing Erk1/2 phosphorylation, we observed that only treatment with UV-irradiated

NVOC-EMP1 induced TrkA dependent signaling in cells expressing EpoR-TrKA (Figure 3.9).

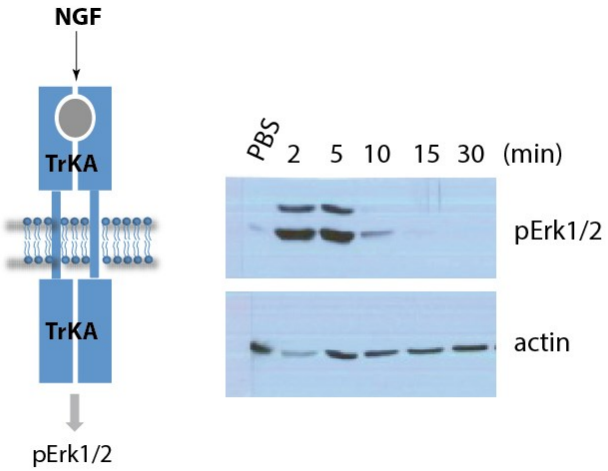

Figure 3.8 NIH3T3 cells were transfected to express full-length TrKA and stimulated with NGF for the indicated times. Activation of TrkA dependent signaling was monitored by the phosphorylation of status of Erk1/2.

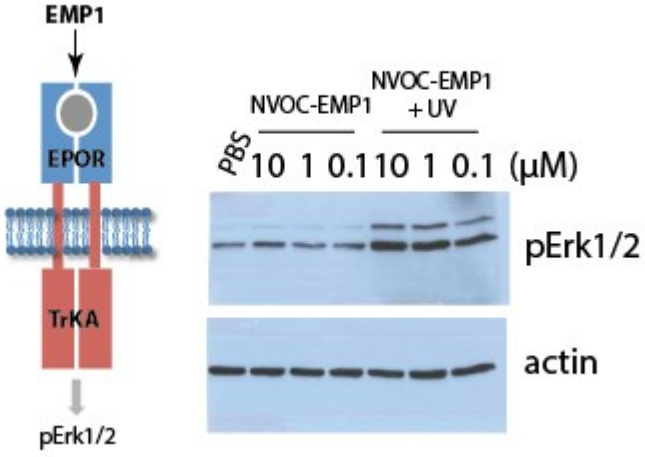

Figure 3.9 NIH-3T3 cells expressing EpoR-TrkA were treated with the indicated concentrations of NVOC-EMP1. TrkA signaling was assessed by immunoblot for phosphorylation of Erk1/2

Using Erk1/2 phosphorylation as the readout for TrKA dependent signaling provided an experimentally robust and rapid way to assess the functionality of the EpoRTrkA system. The MAPK kinases pathway is however only one of the many signaling pathways that gets activated downstream of NGF binding. We wanted to find another assay that allows for a broader assessment of TrKA signaling. The pheochromocytoma cell line PC12, which expresses TrkA, responds to NGF stimulation by adhering to the extracellular matrix and growing extended neurites[111]. We therefore used this PC12 NGF dependent cellular differentiation phenotype as a way to further examine the capacity of NVOC-EMP1 to elicit TrkA signaling in a light inducible manner. Specifically, PC12 cells expressing EpoR-TrkA, upon treatment with NVOC-EMP1, should in a UV-dependent manner undergo TrkA-dependent differentiation. As a control, we needed to first determine that no EpoR-dependent differentiation occurs in these cells. Indeed, Epo dependent neurite outgrowth was not observed in untransfected cells (Figure 3.10A). We next tested the ability of NVOC-EMP1 to activate TrkA dependent signaling. We incubated EpoR-TrkA expressing PC12 cells with NVOC-EMP1 that was either untreated or irradiated with UV light. Only irradiated NVOC-EMP1 induced robust PC12 differentiation (Figure 3.10B), indicating that this ligand is capable of inducing the full complement of TrkA dependent signaling responses in a UV-dependent manner.

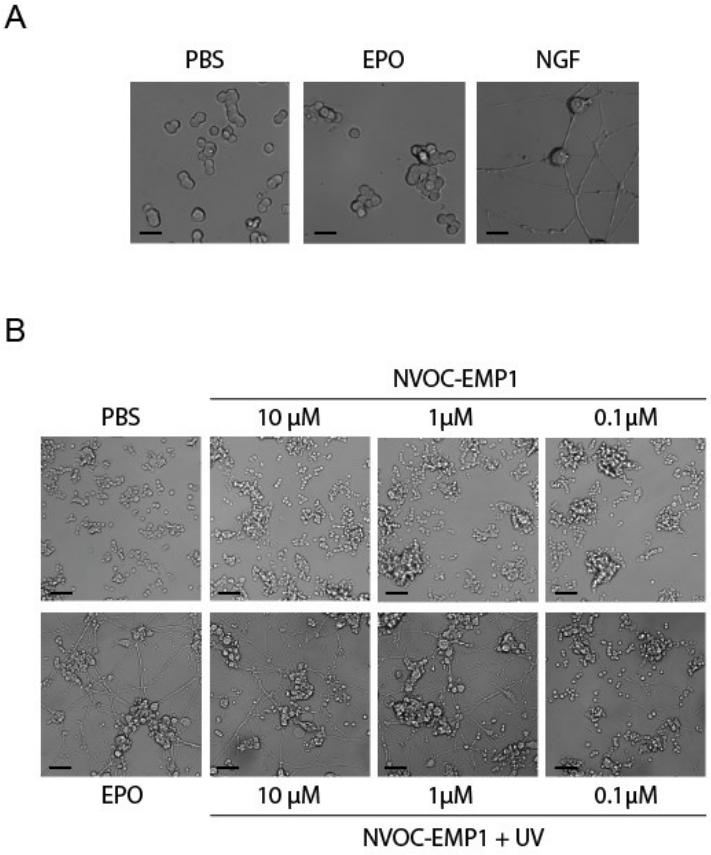

Figure 3.10 EpoR-TrkA signaling induces neurite outgrowth in PC12 cells. (A) PC12 cells were allowed to differentiate on collagen coated tissue culture plates in response to stimulation by EPO (10 ng/mL), NGF (20 ng/mL) or medium at 37^0C for three days. Representative end-point phase contrast images of PC12 cells morphology are shown. Scale bars = 20 µm (B) PC12 cells expressing EpoR-TrkA were stimulated on collagen coated tissue culture plates for three days with medium, EPO (10ng/mL), untreated NVOC-EMP1 or UV-irradiated NVOC-EMP1 at the indicated concentrations. Representative end-point phase contrast images of each condition are shown. Scale bars = 100 µm.

The two receptors, EGFR and TrkA, tested above both belong to the receptor tyrosine kinase superfamily. To further demonstrate the universality of the NVOC-EMP1-EpoR chimeric platform, we asked if our approach could be applied to a receptor outside the RTK family. Toll-like receptor 4 (TLR4) is a single pass transmembrane receptor that gets activated via ligand-induced dimerization. Unlike RTKs however, TLR4 is non catalytic. The receptor plays a crucial role in the innate immune system by mediating cellular responses to its cognate ligand lipopolysaccharide (LPS). That TLR4 engages a lipid ligand is also of interest to us. Designing a caged ligand for LPS would be very difficult due to the chemical complexity of the glycolipid composition. LPS binding of TLR4 induces the transduction of inflammatory signals, some of which are mediated by the adaptor protein MyD88 and the transcription factor NF-κB[112]. The activation of this pathway can be monitored biochemically by the degradation of IκBα, an inhibitory scaffold that sequesters NF-κB in the cytoplasm (Figure 3.11) Using the degradation of IκBα as a biochemical proxy for TLR4-dependent signaling, we next set out to demonstrate that NVOC-EMP1 could be used to drive TLR4 signaling in a UV-dependent manner. We prepared an EpoR-TLR4 chimera and transduced the construct into RAW 264.7 macrophages. Treatment of these cells with UV-irradiated NVOC-EMP1, but not the but not the unirradiated peptide, elicited robust IκBα degradation (Figure 3.12), validating the potential of NVOC-EMP1 to drive UV-dependent signals through EpoR-TLR4.

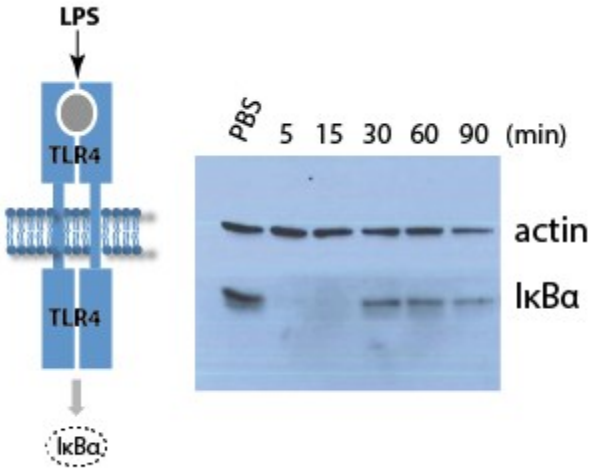

Figure 3.11 TLR4-dependent signaling in RAW 264.7 macrophage cell line. RAW 264.7 macrophages were treated with LPS (1μg/mL) for the indicated times, and IκBα assessed by immunoblot. Actin served as a loading control.

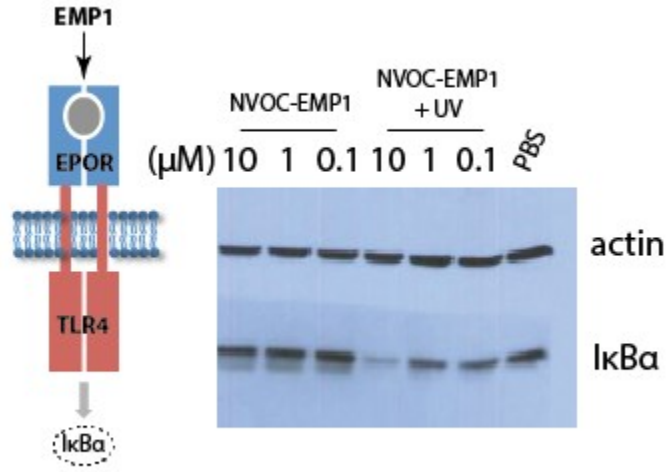

Figure 3.12 RAW 264.7 cells expressing EpoR-TLR4 were treated with the indicated concentrations of NVOC-EMP1.

3.2.4 NVOC-EMP1 can activate receptors in spatiotemporally specific manner.

As outlined in the introduction of this chapter and in scheme 3.1, the goal for developing the NVOC-EMP1-EpoR chimeric system was to implement a videomicroscopy platform, where cell surface receptors could be activated in a spatiotemporally specific manner and the ensuing signaling dynamics could be imaged and quantitatively measured. We therefore set out to determine this very possibility.

Among the three different receptors that we had validated biochemically, TLR4 signaling could be robustly monitored in real time by fluorescently labeling the P65 subunit of NF-κB[113]. LPS stimulation of TLR4 results in the nuclear translocation of this transcription factor. Accordingly, we transduced RAW 264.7 macrophages with GFP- and RFP-tagged forms of P65. Treatment of these cells with LPS induced the translocation of P65-GFP and P65-RFP into the nucleus within 20 minutes, indicative of strong NF-κB signaling (Figure 3.13A. and data not shown.) We also observed this response after applying Epo to RAW 264.7 cells that expressed EpoR-TLR4 (Figure 3.13B.) Importantly, Epo failed to induce NF-κB translocation in cells lacking the chimeric receptor, confirming the specificity of our approach (Figure 3.13C.)

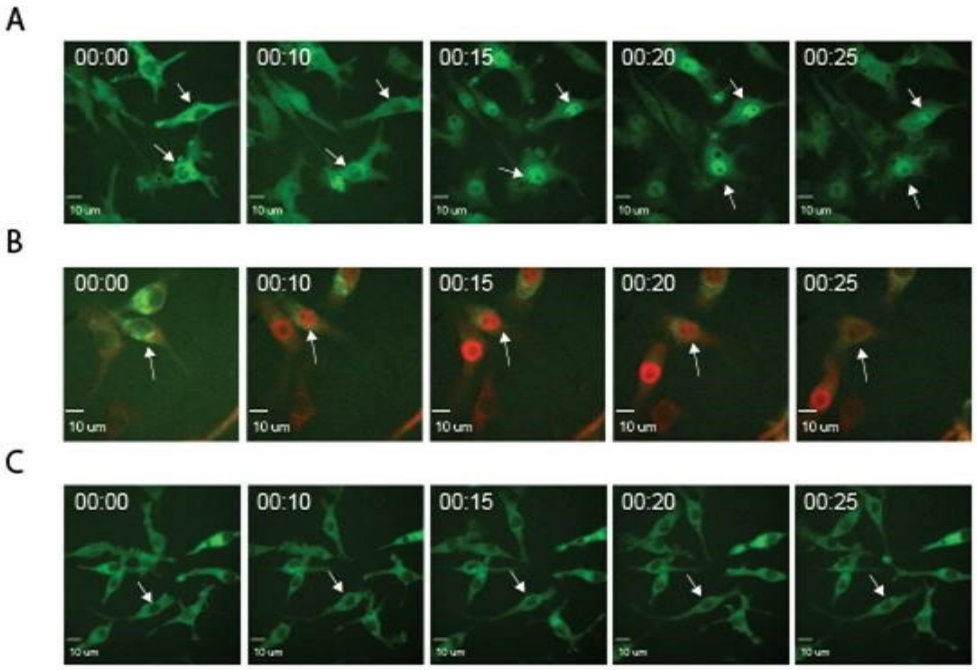

Figure 3.13 EPO can induce TLR4 dependent signaling (p65 nuclear localization) through chimeric receptor EPOR-TLR4. Time-lapse montages show (A) raw cells expressing p65-GFP and stimulated with LPS (1 μg/mL), (B) raw cells expressing EPOR-TLR4-GFP and p65-RFP and stimulated with EPO and (C) raw cells expressing p65-GFP and stimulated with EPO. All stimuli were added at the start of the experiment (Time 00:00). p65 nuclear localization is indicated by white arrows. Scale bars = 10 μm. Time in HH:MM is indicated in the top left corner of each image.

To photoinduce TLR4 signaling during a live imaging experiment, we adhered RAW 264.7 cells expressing EpoR-TLR4-GFP and P65-RFP to glass surfaces coated with NVOC-EMP1, which we immobilized using an established streptavidin-biotin approach[11]. Then, we used a UV light source coupled to an optical digital diaphragm to irradiate the surface beneath a

group of cells. A brief (5 seconds) pulse of UV was sufficient to induce P65 translocation into the nucleus (Figure 3.14A), similar to what we had observed in cells treated with soluble Epo. Importantly, UV irradiation had no effect on P65 localization in the absence of immobilized NVOC-EMP1 (Figure 3.14B), indicating that the translocation response we observed resulted from bona fide TLR4 signaling rather than phototoxicity.

A

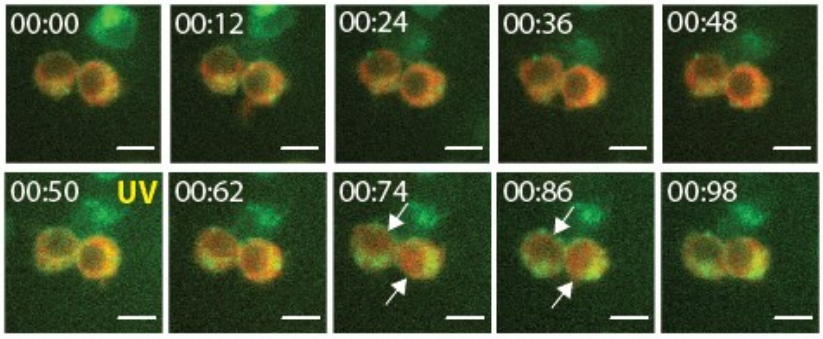

B

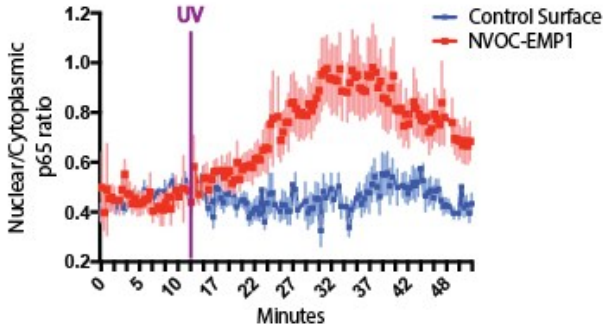

Figure 3.14 A representative time-lapse montage showing translocation of P65-RFP to the nucleus after a 5 second UV pulse, denoted by yellow text. White arrows indicate nuclear localization of P65.

The p65 photoactivation experiment demonstrated that the NVOC-EMP1 platform could photo-induce TLR4 dependent signaling under the microscope. It also highlighted the precise temporal control of TLR4 signaling with the use of UV. What the low-magnification photo-activation experiment did not demonstrate, however, was the extent to which subcellular spatial resolution could be achieved with the NVOC-EMP1 ligand. To highlight the spatial resolution of the platform, we decided to photo-activate EpoR-TLR4 expressing macrophages at a higher magnification where subcellular regions of cells could be selectively irradiated with UV. For these experiments, we used an optical digital diaphragm system to deliver UV light to small regions of the surface beneath individual cells adhered to surface pre-coated with caged ligand. The spatial resolution at which the NVOC-EMP1 platform can stimulate cell surface receptor activation would then depend on the ability of the optical system to decage the immobilized ligand in a spatially precise manner. We therefore needed to first test the system's ability to focus UV light and induce photolysis in a spatially defined way.

5- carboxymethoxy-2-nitrobenzyl (CMNB) carboxyfluorescein is a photo-caged green fluorophore. In its photo-caged form, CMNB carboxyfluorescein fluoresces weakly. Upon UV irradiation which induces photolysis of the CMNB caging group, the decaged carboxyfluorescein recovers its fluorescence. CMNB is chemically similar to NVOC and shares the same mechanism of UV-induced photolysis[114]. Furthermore, efficient and spatially precise de-caging of CMNB carboxyfluorescein would result in a sharp

increase in green fluorescence that is spatially constrained in the region targeted for irradiation. For these reasons, we used CMNB carboxyfluorescein as proxy for NVOC-EMP1 to test the spatial resolution of our irradiation system. The experiment involved coating glass with CMNB carboxyfluorescein and using the digital diaphragm to deliver UV-light onto regions of various sizes. We found that the system can achieve clean and uniform decaging of circular areas less than 5 μm in diameter (Fig. 3.15).

Finally, having confirmed the spatial precision of our irradiation apparatus, we set out to photo-activate EpoR-TLR4. To assess TLR4 activation, we relied on the receptor's known activation-induced oligomerization. Previous studies have shown that TLR4 undergoes rapid oligomerization within minutes of ligand binding, forming clusters on the plasma membrane that persist for up to 50 minutes[115,116]. Since the EpoRTLR4 expression construct contains a fluorescent eGFP protein at the C-terminus, clustering at the membrane as a result of TLR4 dependent signaling could be easily imaged and quantified. Accordingly, we adhered RAW cells expressing EpoRTLR4 onto a glass surface pre-coated with NVOC-EMP1. We used total internal

reflection fluorescence (TIRF) imaging to record signaling events at the plasma membrane.

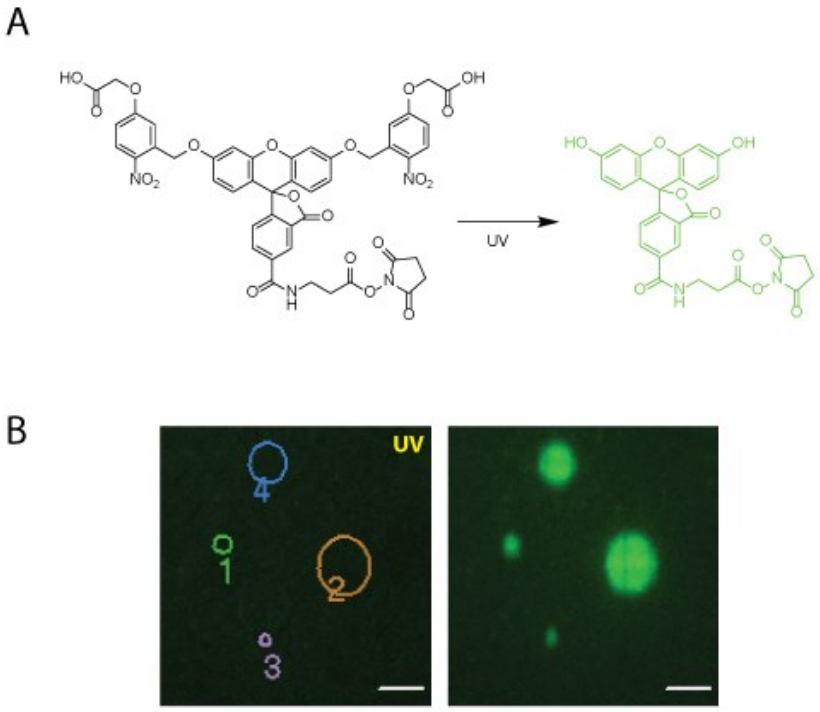

Figure 3.15. Constrained decaging by the Mosaic digital diaphragm. (A) Reaction diagram showing UV decaging of 5- carboxymethoxy-2-nitrobenzyl (CMNB) carboxyfluorescein. (B) Glass surfaces coated with immobilized CMNB carboxyfluorescein were subjected to focused UV irradiation. Representative images taken before and after decaging are shown, with the region of UV irradiation indicated by the circles to the left. Scale bars = 10 μm.

Using the digital diaphragm system, we irradiated a subcellular region on a cell. Irradiation in this manner induced rapid clustering of EpoR-TLR4-GFP (Fig. 3.16). Importantly, cluster formation was significantly more pronounced

within the irradiated region, demonstrating that NVOC-EMP1 can be used in conjunction with focused UV light to elicit signaling responses in the plasma membrane with spatial precision. As a control for UV-toxicity, we irradiated EpoT-TLR4 expressing cells on glass surface with no caged ligand. This response was not observed in the absence of NVOC-EMP1 which indicates that it resulted specifically from ligand engagement by EpoR-TLR4-GFP (Fig. 3.17).

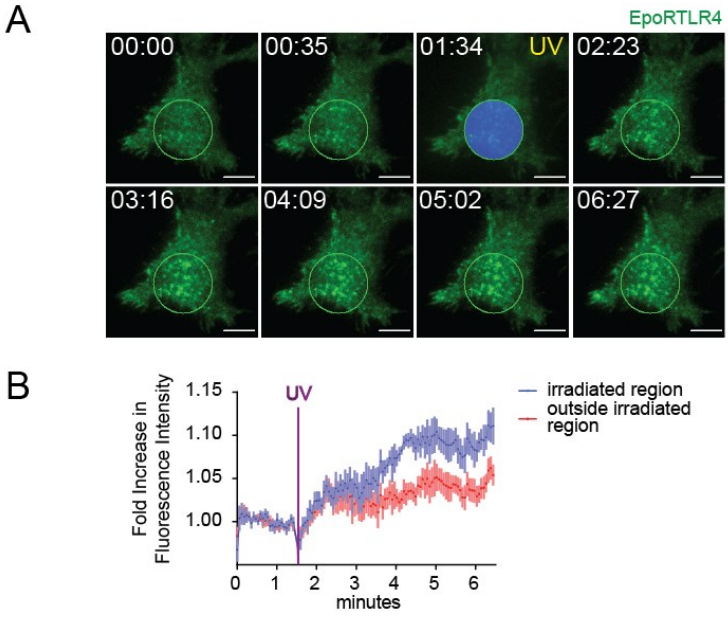

Figure 3.16. Constrained NVOC-EMP1 photoactivation can be used to elicit localized signaling responses. RAW 264.7 cells expressing EpoR-TLR4-GFP were imaged and UV-irradiated on glass surfaces coated with NVOC-EMP1. epresentative time-lapse montage showing receptor cluster formation after UV activation

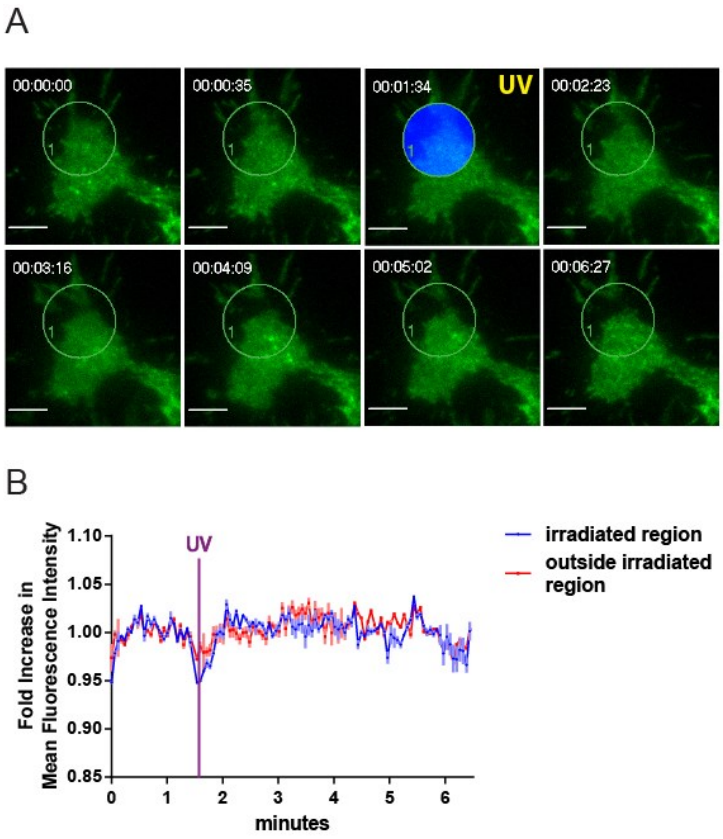

Figure 3.17. UV alone does not induce clustering of EpoR-TLR4. RAW 264.7 cells expressing EpoR-TLR4-GFP were imaged and UV-irradiated on glass surfaces without NVOC-EMP1. (A) Time-lapse montage of a representative experiment, with the region of irradiation (3 s pulse) denoted by the green circle and the time of irradiation by yellow text. Time in HH:MM:SS is indicated in the top left corner of each image. Scale bars = 5 μm. (B) Quantification of experiment shown in (A). Cluster formation was quantified by calculating the normalized mean fluorescence intensity inside and outside the irradiated region. UV irradiation is indicated by the purple line. Error bars denote s.e.m. Data are representative of two independent experiments (n≥10 cells per condition).

3.3 DISCUSSION

In summary, we have established NVOC-EMP1 as a generalizable platform for the photoactivation of a wide range of receptor signaling pathways. We have also validated the potential of this molecule to elicit pathway specific signaling responses in real time during videomicroscopy experiments with both spatial and temporal specificity. The application of NVOC-EMP1 together with EpoR chimeras circumvents the time consuming process of engineering distinct photocaged ligands for each receptor of interest. Many receptor ligands are large polypeptides, lipoproteins, or glycolipids, which present formidable design and synthesis problems. By contrast, NVOC-EMP1 is a small peptide that can be produced in large quantities via standard solid phase peptide chemistry.

3.4 MATERIALS and METHODOLOGY:

General Methods and Reagents. Erythropoietin was purchased from eBiosciences, nerve growth factor (NGF) and epidermal growth factor (EGF) from Invitrogen, and liposaccharide (LPS) from Sigma Aldrich. PCR primers and templates were purchased from Integrated DNA Technologies. Unless otherwise indicated, all expression plasmids were purchased from Addgene. Fmoc-protected amino acids were obtained from Merck Millipore, and all other chemicals used in solid phase peptide synthesis were purchased from Sigma Aldrich. Synthesis grade organic solvents were from Fisher Scientific. Peptide purification and small molecule purification were carried out using an HPLC system (Waters) outfitted with a C18 reversed phase column (VYDAC.) Mass spectrometry data was obtained by LC-MS (Agilent

Technologies) at the Memorial Sloan Kettering Cancer Center Mass Spectrometry Core Facility.

Compound Synthesis and Purification. Fmoc-Tyr(NVOC)-OH was synthesized as described previously[117]. NVOC-EMP1 was synthesized by standard Fmoc Solid Phase Peptide Synthesis (SPPS) on Rink Amide resin. SPPS reactions were carried out in a custom-made glass peptide synthesis vessel (Adams & Chittenden). A constant stream of nitrogen was used to provide gentle agitation. Amino acid coupling was performed using HBTU as the carboxylic acid activating agent and DIPEA as the organic base in DMF solvent. For each coupling reaction: 3 eq of FMOC-AA-OH, 2.9 eq of HBTU and 3 eq of DIPEA were used. Coupling time was one hour at room temperature. Deprotection of FMOC was performed with 20% Piperidine/DMF for 20 minutes. The full sequence of NVOC-EMP1 is as follows: GGTY(NVOC) SCHF GPLT WVCK PQGG SSK(Biotin). Synthetic details are outlined in Supplemental Scheme 1. Assembled NVOC-EMP1 was globally deprotected and cleaved from the resin using neat trifluoroacetic acid containing 5% water, 5% phenol, 5% thioanisole, and 2.5% 1,2-ethanedithiol. The peptide was then purified by HPLC using a water/acetonitrile gradient, yield: 10%. $[M+H]^{3+}$ calculated for $C_{125}H_{180}N_{32}O_{37}S_3$ was 940.083; found 940 (Fig. S1). Disulfide bond formation was induced by dissolving NVOC-EMP1 in 10% DMSO/phosphate buffered saline (PBS) and exposing the solution to air overnight. The folded peptide was subsequently stored at 4^0C in 10%DMSO/PBS.

Construction of Expression Plasmids. EpoR chimeras were constructed by fusing the extracellular and transmembrane domains of mouse EpoR (amino acids 1-271) to the intracellular domain of the receptor of interest via stitching PCR. The EpoR-EGFR construct contains amino acids 668-1210 of human EGFR; the EpoR-TrkA construct contains amino acids 441-799 of rat TrkA; the EpoR-TLR4 construct contains amino acids 625-835 of mouse TLR4. cDNA encoding full-length rat TrkA was a gift from the Marc Tessier-Lavigne lab (Rockefeller University). EpoR chimeras were cloned into the *AgeI* or *BamHI* sites of the lentiviral expression vector pRRL eGFP (Addgene) upstream of the GFP coding sequence. p65 cDNA was amplified via reverse-transcription from RNA extracted from B6 Mouse liver and cloned into pRRL RFP using the *AgeI* restriction site upstream of the RFP coding sequence. The pRRL RFP expression vector was modified from the parental pRRL eGFP by subcloning cDNA coding for the monomeric red-fluorescence protein TagRFP-T into the *AgeI* and *SalI* sites.

Cell Culture and Lentiviral Transduction. NIH-3T3 and RAW 264.7 (both from American Type Culture Collection) were maintained in complete DMEM supplemented with 10% fetal bovine serum (FBS) and antibiotics. PC12 cells (ATCC) were maintained in complete RPMI media supplemented with 10% Horse Serum, 5% FBS, and antibiotics. TF1 cells (ATCC) were maintained in complete RPMI media supplemented with 10% Horse Serum and 5% FBS, antibiotics and 2 ng/mL of human GM-CSF. Lentiviral transduction was carried out with second-generation lentiviral packaging plasmids psPAX2 and pMD2.G (Addgene). HEK293HF cells (ATCC) at about 90% confluency

were transfected with the aforementioned lentiviral packaging plasmids by calcium phosphate method. Viral supernatants were collected after 48 hr at 37^0C and were added to 50% confluent NIH-3T3 and RAW 264.7 cells or to 2 million PC12 cells in suspension. Mixtures were subsequently centrifuged at 1000 × g in the presence of polybrene (4 μg/mL) at 35^0C for 1 hr and allowed to incubate overnight at 37^0C. Cells were then expanded in fresh medium.

Biochemical Assays/Western Blotting. Approximately 2×10^5 cultured cells were used for each gel sample in signaling experiments. NVOC-EMP1 was decaged by UV irradiation on ice for 45 minutes using a handheld lamp outfitted with a 6 Watt 350 nm light source. Prior to ligand stimulation, cultured cells were starved of serum and other growth factors for two hours. After ligand treatment, cells were lysed in cold cell lysis buffer containing 10 mM TrisHCl, pH 7.4, 5 mM EDTA, 1% NP-40, 0.5% sodium deoxycholate, and 0.15 M NaCl. Samples were then analyzed by western blot using the following antibodies: P-Erk1/2 (P-Thr202/Tyr204; clone 20G11; Cell Signaling Technology), P-EGFR (P-Tyr 1068; clone 2234; Cell Signaling Technology), IκBα (clone 9242; Cell Signaling Technology), actin (clone AC40; Sigma Aldrich), mouse IgG HRP-linked (clone 7076, Cell Signaling Technology), rabbit IgG HRP-linked (clone 7074; Cell Signaling Technology). Each antibody was used at the manufacturer's recommended dilution.

Neuronal Differentiation Assay. Actively dividing PC12 cells were treated with trypsin for 15 min at 37^0C to create single cell suspensions. Cells were

then plated onto 24-well tissue culture plates ($1x10^4$ per well) that had been previously coated with 40 µg/ml of rat tail collagen Type I (Sigma Aldrich) in RPMI supplemented with 2.5% horse serum. NGF, Epo, or NVOC-EMP1 was added at desired concentrations and cells were allowed to incubate for 3 days at 37^0C before imaging analysis.

Photoactivation and Fluorescence Microscopy Experiments. Glass surfaces for photoactivation were prepared from eight-well chamber slides (Nunc). Chamber slides were coated with biotinylated poly-L-lysine (produced with NHS-biotin, Pierce Biotechnology), washed with H_2O, and allowed to dry overnight. They were then incubated with streptavidin (100 µg/mL in PBS) for at least 1 hr. After washing with PBS, the surfaces were incubated in the desired concentration of biotinylated NVOC-EMP1 for 1 hr in PBS. They were washed again and left in PBS until use. RAW 264.7 cells were allowed to adhere to coated chamber slides for 10 min at 37^0C before data collection. Live imaging experiments were carried out using an inverted fluorescence video microscope fitted with either a 40 × objective lens or 150 × TIRF objective lens (Olympus). Lasers at 488 nm and 561 nm (Melles Griot) were used for imaging of GFP and TagRFP-T, respectively. A Mosaic digital diaphragm apparatus (Photonic Instruments) attached to a mercury (HBO) lamp (serial number: Ushio USH-102DH, 100 Watts, 20 Volts) was used for photoactivation. The approximate UV intensity given the microscope set up in our laboratory is 1 mW/cm^2. Time-lapse recordings were made with Slidebook software (Intelligent Imaging Innovations). For p65 nuclear localization experiments, images were acquired every 20 s. For TIRF

photoactivation experiments, images were acquired every 3 s. Cells were activated with a UV exposure of 3-5 s.

Image Analysis. Nuclear localization of P65 was quantified ratiometrically by determining the average p65-RFP fluorescence intensity in the nucleus at each time point and dividing this by the p65-RFP fluorescence intensity of a corresponding region in the cytosol. EpoR-TLR4-GFP accumulates in perinuclear compartments as well as the cell membrane, enabling straightforward identification of the nucleus in the GFP channel as a central region devoid of GFP fluorescence. EpoR-TLR4-GFP clustering was quantified by determining the mean fluorescence intensity of the cell footprint inside and outside of the irradiated region as a function of time. Image analysis was performed using Slidebook, Microsoft Excel, and GraphPad Prism.

CONCLUSIONS

The two technologies described in this thesis have much potential to be expanded upon as video-microscopy platforms to study polarized signal transduction.

As discussed in chapter 1, current light-gated approaches to activate cell surface receptors rely on the intracellular expression of light sensitive proteins, which can diffuse to other parts of the cell after photo-stimulation. Because NVOC-EMP1 can be immobilized outside of the cell, it provides a more straightforward avenue for the induction of signaling that is both sustained and spatially constrained. We anticipate that this property will be very useful for the study of signaling systems that provide directional information. Axon guidance, for example, is mediated by cell surface receptors that translate environmental cues into turning behavior; attractive factors induce polarized cytoskeletal outgrowth toward them, while repulsive factors cause localized cytoskeletal collapse and retraction[94]. Because these responses can take up to an hour to manifest, an experimental system that maintains polarity over this timescale will presumably be critical for detailed mechanistic analyses. The NVOC-EMP1 platform should also be useful for studying receptors that function in multiple cellular compartments. TLR4, for instance, transduces qualitatively different signals depending on whether it is activated at the plasma membrane or in endosomes[118]. By selectively targeting receptors on the plasma membrane, our approach will enable investigators to delineate these two branches of the signaling cascade

The NVOC-EMP1 platform suffers from a few drawbacks. The most obvious is associated with the use of chimeric receptors. Replacing the extracellular domain of a receptor with that of another poses the risk that some, if not all functionalities, of the original receptor will be negatively affected. We indeed saw such effects on CSF1R, a type I trans-membrane receptor tyrosine kinase important for macrophage differentiation and chemotaxis. The EpoR-CSF1R chimeric receptor only recapitulates some of the signaling circuits downstream of CSF1R activation (Data not shown). It is therefore necessary to fully test the functionality of EpoR-chimeric receptors.

Another potential drawback stems from the use of EpoR as the parent receptor from which chimeras are derived. We chose to work with EpoR for the reason that it is one of the better-characterized receptors. Furthermore, that EMP1, a small peptide, had been developed as a functional mimic of the full length Epo ligand, simplified the design of a caged agonist. Our strategy rests on the assumption that EpoR is a specialized receptor whose expression is limited to cells in the erythroid lineage. While EpoR expression is mostly absent in epithelial and cancer cell lines (NIH3T3, HEK293T and RAW 264.7), EpoR has recently been shown to be expressed in cells of the myeloid and lymphoid lineage[119]. Expression of EpoR-chimeric receptors in cells expressing endogenous EpoR could prove to be problematic, especially if the endogenous EpoR signaling interferes with that of the EpoR-chimeric receptor. Recent advances in genome editing technologies, such as CRISPR, provide a work-around. Endogenous EpoR could be deleted in the genome of the cell of interest where necessary.

NVOC-EMP1 is the first universal ligand platform of its kind to activate cell surface receptors in a light-dependent manner. Looking forward, the system holds tremendous promise for detailed mechanistic studies of cell surface receptor signaling at high spatiotemporal resolution. Given the need to create chimeras, there are a few key considerations in the selection of cell surface receptors that are to be studied using the NVOC-EMP1 platform. From a functional perspective, as has been discussed above, EPOR-chimeric receptors are not guaranteed to be fully functional and extensive testing therefore is necessary to validate the functionality of chimeras of interest. To increase the likelihood of creating fully functional EPOR-chimeras, receptors that share similar structural and activation features to those of EPOR would be good candidates. As EPOR belongs to the cytokine receptor family, cytokine receptors would likely form functional EPOR-chimeras. Indeed, a fully functional chimeric receptor consisting of the extracellular domain of EPOR and transmembrane and intracellular domains of IFN-γ has been previously described[120]. Receptor tyrosine kinases, whose activation mechanism relies on ligand-induced dimerization of homodimer receptors, should in theory be good candidates for EPOR-chimeras. Indeed, functional EPOR chimeras of EGFR (described in chapter 3) and stem cell factor (SCF) receptor have been successfully created[103]. CSF1R as previously discussed is a noteworthy exception, which once again highlights the need to extensively test EPOR-chimeras for functionality.

The other consideration when selecting receptors for investigation using the NVOC-EMP1 platform takes into account the biological significance of the associated downstream signaling. The NVOC-EMP1 system was designed

to provide a means to control activation of cell surface receptors in a spatiotemporal specific manner. Such precise control is uniquely suited for the analysis of polarized signal transduction from cell surface receptors. Receptors with known polarized signal transduction such as TrkA are therefore attractive candidates. Other receptors, such as TLR4 whose signaling dynamics upon activation remain incompletely understood, yet might be implicated in polarized signal transduction, are also attractive candidates for further investigation using the NVOC-EMP1 platform.

Devoid of all the drawbacks associated with use of EPOR-chimeric receptors, the photoactivatable SDF1α system makes use of a native ligand to activate an endogenously expressed receptor. Current light-gated technologies to control chemokine receptor activation require cellular expression of a light sensitive chimeric GPCR[45,46]. Since primary cells such as stem cells and neutrophils are notoriously difficult to manipulate genetically without altering their stemness or activation status respectively, the use of a native light-gated ligand capable of activating endogenous receptor is therefore a tremendous advantage.

That NVOC-SDF1α is a native ligand also facilitates the extension of the system to *in vivo* studies. For example, SDF1α has long been appreciated as a key chemokine that mediates the recruitment of CXCR4 positive tumor promoting macrophages (TAMs) into the tumor microenvironment. The chemokine was also shown to be important in the recruitment of endothelial progenitors which promote tumor angiogenesis[121]. Caged SDF1α provides a means to study such recruitment dynamics in the tumor microenvironment

with spatial and temporal resolution. Since the caged chemokine is inactive until photo-activated, it can be delivered to the tumor sites via the circulatory system or direct injection into the tumors. Modification of the caging group would have to be made to accommodate for two-photon de-caging, but in principle, the caged chemokine would serve as a useful tool to study the recruitment dynamics of a wide range of cell types in the tumor microenvironment.

NVOC-SDF1α highlights the central role that the unstructured N-terminal domain plays in the functionality of the full protein and how such a structural property could be exploited to create a photo-caged ligand. Interestingly, SDF1α or CXCL12 is not the only chemokine to contain such unique functionality within the N-terminal residues. Studies of the chemokines CCL2, CCL5, CCL19, and CXCL10 have all revealed a critical role for the N-terminal residues in controlling the chemokines' agonist activity[18]. This structural feature then provides a general strategy to generate caged chemokines. Indeed, as this thesis was being written, a photoactivatable CCL5 chemokine was generated by photo-caging key residues in the chemokine's N-terminal domain[122]. That caged chemokines can be generated with relative ease using a common strategy (i.e.: photo-caging the N-terminal domain) holds great promise for mechanistic studies of the biology of chemokines and chemokine receptors.

Biological processes harbor tremendous complexity. For example, as discussed at length in the previous chapters of this thesis, a single event of ligand binding to a cell surface receptor triggers a plethora of downstream

reactions and enzymatic circuits that often interact with each other in space and time to drive cellular events. Such complexity renders the study of biology one that relies heavily on advances in technology that allow for careful measurements to be made. This thesis described two attempts to provide biologists with tools to make careful and quantitative observations from which biological processes could be better understood.

REFERENCES

(1) Kaplan, J. H., Forbush, B., and Hoffman, J. F. (1978) Rapid photolytic release of adenosine 5’-triphosphate from a protected analog - utilization by Na-K pump of human red blood-cell ghosts. *Biochemistry 17*, 1929–1935.

(2) Engels, J., and Schlaeger, E. J. (1977) Synthesis, structure, and reactivity of adenosine cyclic 3’,5'-phosphate benzyl triesters. *J. Med. Chem. 20*, 907–911.

(3) Mayer, G., and Hechel, A. (2006) Biologically active molecules with a “light switch.” *Angew. Chemie - Int. Ed. 45*, 4900–4921.

(4) Callaway, E. M., and Yuste, R. (2002) Stimulating neurons with light. *Curr. Opin. Neurobiol. 12*, 587–592.

(5) Marriott, G. (1998) Methods in Enzymology. *Methods Enzymol.* Academic Press, San Diego.

(6) Smith, M. a, Ellis-Davies, G. C. R., and Magee, J. C. (2003) Mechanism of the distance-dependent scaling of Schaffer collateral synapses in rat CA1 pyramidal neurons. *J. Physiol. 548*, 245–258.

(7) Matsuzaki, M., Ellis-Davies, G. C., Nemoto, T., Miyashita, Y., Iino, M., and Kasai, H. (2001) Dendritic spine geometry is critical for AMPA receptor expression in hippocampal CA1 pyramidal neurons. *Nat. Neurosci. 4*, 1086–1092.

(8) Kurahashi, T., and Menini, a. (1997) Mechanism of odorant adaptation in the olfactory receptor cell. *Nature*.

(9) Nadler, A., Reither, G., Feng, S., Stein, F., Reither, S., Müller, R., and Schultz, C. (2013) The fatty acid composition of diacylglycerols determines local signaling patterns. *Angew. Chemie - Int. Ed. 52*, 6330–6334.

(10) DeMond, A. L., Starr, T., Dustin, M. L., and Groves, J. T. (2006) Control of antigen presentation with a photoreleasable agonist peptide. *J. Am. Chem. Soc. 128*, 15354–15355.

(11) Huse, M., Klein, L. O., Girvin, A. T., Faraj, J. M., Li, Q.-J., Kuhns, M. S., and Davis, M. M. (2007) Spatial and temporal dynamics of T cell receptor signaling with a photoactivatable agonist. *Immunity 27*, 76–88.

(12) Quann, E. J., Merino, E., Furuta, T., and Huse, M. (2009) Localized diacylglycerol drives the polarization of the microtubule-organizing center in T cells. *Nat. Immunol. 10*, 627–35.

(13) Quann, E. J., Liu, X., Altan-Bonnet, G., and Huse, M. (2011) A cascade of protein kinase C isozymes promotes cytoskeletal polarization in T cells. *Nat. Immunol. 12*, 647–654.

(14) Liu, X., Kapoor, T. M., Chen, J. K., and Huse, M. (2013) Diacylglycerol promotes centrosome polarization in T cells via reciprocal localization of dynein and myosin II. *Proc. Natl. Acad. Sci. U. S. A. 110*, 11976–81.

(15) Abeyweera, T. P., Merino, E., and Huse, M. (2011) Inhibitory signaling blocks activating receptor clustering and induces cytoskeletal retraction in natural killer cells. *J. Cell Biol. 192*, 675–90.

(16) Toebes, M., Coccoris, M., Bins, A., Rodenko, B., Gomez, R., Nieuwkoop, N. J., van de Kasteele, W., Rimmelzwaan, G. F., Haanen, J. B. a G., Ovaa, H., and Schumacher, T. N. M. (2006) Design and use of conditional MHC class I ligands. *Nat. Med. 12*, 246–251.

(17) Huse, M. (2010) Photochemical approaches to T-cell activation. *Immunology 130*, 151–7.

(18) Allen, S. J., Crown, S. E., and Handel, T. M. (2007) Chemokine: receptor structure, interactions, and antagonism. *Annu. Rev. Immunol. 25*, 787–820.

(19) Hoppe, U. C., Marbán, E., and Johns, D. C. (2000) Adenovirus-mediated inducible gene expression in vivo by a hybrid ecdysone receptor. *Mol. Ther. 1*, 159–164.

(20) Kistner, a, Gossen, M., Zimmermann, F., Jerecic, J., Ullmer, C., Lübbert, H., and Bujard, H. (1996) Doxycycline-mediated quantitative and tissue-specific control of gene expression in transgenic mice. *Proc. Natl. Acad. Sci. U. S. A. 93*, 10933–10938.

(21) Lin, W., Albanese, C., Pestell, R. G., and Lawrence, D. S. (2002) Spatially discrete, light-driven protein expression. *Chem. Biol. 9*, 1347–1353.

(22) Cambridge, S. B., Geissler, D., Calegari, F., Anastassiadis, K., Hasan, M. T., Stewart, a F., Huttner, W. B., Hagen, V., and Bonhoeffer, T. (2009) Doxycycline-dependent photoactivated gene expression in eukaryotic systems. *Nat. Methods 6*, 527–531.

(23) Umeda, N., Ueno, T., Pohlmeyer, C., Nagano, T., and Inoue, T. (2011) A photocleavable rapamycin conjugate for spatiotemporal control of small GTPase activity. *J. Am. Chem. Soc. 133*, 12–14.

(24) Karginov, A. V., Zou, Y., Shirvanyants, D., Kota, P., Dokholyan, N. V., Young, D. D., Hahn, K. M., and Deiters, A. (2011) Light regulation of protein dimerization and kinase activity in living cells using photocaged rapamycin and engineered FKBP. *J. Am. Chem. Soc. 133*, 420–423.

(25) Sinha, D. K., Neveu, P., Gagey, N., Aujard, I., Benbrahim-Bouzidi, C., Le Saux, T., Rampon, C., Gauron, C., Goetz, B., Dubruille, S., Baaden, M., Volovitch, M., Bensimon, D., Vriz, S., and Jullien, L. (2010) Photocontrol of protein activity in cultured cells and zebrafish with one- and two-photon illumination. *ChemBioChem 11*, 653–663.

(26) Sinha, D. K., Neveu, P., Gagey, N., Aujard, I., Le Saux, T., Rampon, C., Gauron, C., Kawakami, K., Leucht, C., Bally-Cuif, L., Volovitch, M., Bensimon, D., Jullien, L., and Vriz, S. (2010) Photoactivation of the CreER T2 recombinase for conditional site-specific recombination with high spatiotemporal resolution. *Zebrafish 7*, 199–204.

(27) Link, K. H., Shi, Y., and Koh, J. T. (2005) Light activated recombination. *J. Am. Chem. Soc. 127*, 13088–13089.

(28) Hughes, J. (2013) Phytochrome cytoplasmic signaling. *Annu. Rev. Plant Biol. 64*, 377–402.

(29) Ni, M., Tepperman, J. M., and Quail, P. H. (1999) Binding of phytochrome B to its nuclear signalling partner PIF3 is reversibly induced by light. *Nature 400*, 781–784.

(30) Levskaya, A., Weiner, O. D., Lim, W. a, and Voigt, C. a. (2009) Spatiotemporal control of cell signalling using a light-switchable protein interaction. *Nature 461*, 997–1001.

(31) Toettcher, J. E., Gong, D., Lim, W. a, and Weiner, O. D. (2011) Light-based feedback for controlling intracellular signaling dynamics. *Nat. Methods 8*, 837–839.

(32) Banghart, M., Borges, K., Isacoff, E., Trauner, D., and Kramer, R. H. (2004) Light-activated ion channels for remote control of neuronal firing. *Nat. Neurosci. 7*, 1381–1386.

(33) Volgraf, M., Gorostiza, P., Numano, R., Kramer, R. H., Isacoff, E. Y., and Trauner, D. (2006) Allosteric control of an ionotropic glutamate receptor with an optical switch. *Nat. Chem. Biol. 2*, 47–52.

(34) Janovjak, H., Szobota, S., Wyart, C., Trauner, D., and Isacoff, E. Y. (2010) A light-gated, potassium-selective glutamate receptor for the optical inhibition of neuronal firing. *Nat. Neurosci. 13*, 1027–1032.

(35) Gautier, A., Nguyen, D. P., Lusic, H., An, W., Deiters, A., and Chin, J. W. (2010) Genetically encoded photocontrol of protein localization in mammalian cells - Supporting Information *16*, 1–19.

(36) Hemphill, J., Chou, C., Chin, J. W., and Deiters, A. (2013) Genetically Encoded Light-Activated Transcription for Spatiotemporal Control of Gene Expression and Gene Silencing in Mammalian Cells.

(37) Gautier, A., Deiters, A., and Chin, J. W. (2011) Light-activated kinases enable temporal dissection of signaling networks in living cells. *J. Am. Chem. Soc. 133*, 2124–2127.

(38) Nguyen, D. P., Mahesh, M., Elsässer, S. J., Hancock, S. M., Uttamapinant, C., and Chin, J. W. (2014) Genetic encoding of photocaged cysteine allows photoactivation of TEV protease in live mammalian cells. *J. Am. Chem. Soc. 136*, 2240–2243.

(39) Zhang, F., Vierock, J., Yizhar, O., Fenno, L. E., Tsunoda, S., Kianianmomeni, A., Prigge, M., Berndt, A., Cushman, J., Polle, J., Magnuson, J., Hegemann, P., and Deisseroth, K. (2011) The microbial opsin family of optogenetic tools. *Cell 147*, 1446–1457.

(40) Konermann, S., Brigham, M. D., Trevino, A. E., Hsu, P. D., Heidenreich, M., Cong, L., Platt, R. J., Scott, D. a, Church, G. M., and Zhang, F. (2013)

Optical control of mammalian endogenous transcription and epigenetic states. *Nature 500*, 472–6.

(41) Fenno, L., Yizhar, O., and Deisseroth, K. (2011) The development and application of optogenetics. *Annu. Rev. Neurosci. 34*, 389–412.

(42) Fenno, L., Yizhar, O., and Deisseroth, K. (2011) The development and application of optogenetics. *Annu. Rev. Neurosci. 34*, 389–412.

(43) Arrenberg, A. B., Stainier, D. Y. R., Baier, H., and Huisken, J. (2010) Optogenetic control of cardiac function. *Science 330*, 971–974.

(44) Stroh, A., Tsai, H. C., Wang, L. P., Zhang, F., Kressel, J., Aravanis, A., Santhanam, N., Deisseroth, K., Konnerth, A., and Schneider, M. B. (2011) Tracking stem cell differentiation in the setting of automated optogenetic stimulation. *Stem Cells 29*, 78–88.

(45) Airan, R. D., Thompson, K. R., Fenno, L. E., Bernstein, H., and Deisseroth, K. (2009) Temporally precise in vivo control of intracellular signalling. *Nature 458*, 1025–9.

(46) Xu, Y., Hyun, Y.-M., Lim, K., Lee, H., Cummings, R. J., Gerber, S. a, Bae, S., Cho, T. Y., Lord, E. M., and Kim, M. (2014) Optogenetic control of chemokine receptor signal and T-cell migration. *Proc. Natl. Acad. Sci. U. S. A. 111*, 6371–6.

(47) Iseki, M., Matsunaga, S., Murakami, A., Ohno, K., Shiga, K., Yoshida, K., Sugai, M., Takahashi, T., Hori, T., and Watanabe, M. (2002) A blue-light-

activated adenylyl cyclase mediates photoavoidance in Euglena gracilis. *Nature 415*, 1047–1051.

(48) Schröder-Lang, S., Schwärzel, M., Seifert, R., Strünker, T., Kateriya, S., Looser, J., Watanabe, M., Kaupp, U. B., Hegemann, P., and Nagel, G. (2007) Fast manipulation of cellular cAMP level by light in vivo. *Nat. Methods 4*, 39–42.

(49) Edgett, K. S., Moore, H. J., Kieffer, H. H., Jakosky, B. M., Snyder, C. W., and Matthews, M. S. (2008) Photoexcited CRY2 Interacts with CIB1 to Regulate Transcription and Floral Initiation in Arabidopsis. *Science (80-.). 322*, 1535–1539.

(50) Tischer, D., and Weiner, O. D. (2014) Illuminating cell signalling with optogenetic tools. *Nat Rev Mol Cell Biol 15*, 551–558.

(51) Kennedy, M. J., Hughes, R. M., Peteya, L. a, Schwartz, J. W., Ehlers, M. D., and Tucker, C. L. (2010) Rapid blue-light-mediated induction of protein interactions in living cells. *Nat. Methods 7*, 973–975.

(52) Lee, S., Park, H., Kyung, T., Kim, N. Y., Kim, S., Kim, J., and Heo, W. Do. (2014) Reversible protein inactivation by optogenetic trapping in cells. *Nat. Methods 11*, 633–6.

(53) Bugaj, L. J., Spelke, D. P., Mesuda, C. K., Varedi, M., Kane, R. S., and Schaffer, D. V. (2015) Regulation of endogenous transmembrane receptors through optogenetic Cry2 clustering. *Nat. Commun. 6*, 6898.

(54) Chang, K.-Y., Woo, D., Jung, H., Lee, S., Kim, S., Won, J., Kyung, T., Park, H., Kim, N., Yang, H. W., Park, J.-Y., Hwang, E. M., Kim, D., and Heo, W. Do. (2014) Light-inducible receptor tyrosine kinases that regulate neurotrophin signalling. *Nat. Commun. 5*, 4057.

(55) Huala, E., Oeller, P. W., Liscum, E., Han, I. S., Larsen, E., and Briggs, W. R. (1997) Arabidopsis NPH1: a protein kinase with a putative redox-sensing domain. *Science 278*, 2120–2123.

(56) Möglich, A., and Moffat, K. (2010) Engineered photoreceptors as novel optogenetic tools. *Photochem. Photobiol. Sci. 9*, 1286–1300.

(57) Salomon, M., Christie, J. M., Knieb, E., Lempert, U., and Briggs, W. R. (2000) Photochemical and mutational analysis of the FMN-binding domains of the plant blue light receptor, phototropin. *Biochemistry 39*, 9401–9410.

(58) Pudasaini, A., El-Arab, K. K., and Zoltowski, B. D. (2015) LOV-based optogenetic devices: light-driven modules to impart photoregulated control of cellular signaling. *Front. Mol. Biosci. 2*, 1–15.

(59) Swartz, T. E., Corchnoy, S. B., Christie, J. M., Lewis, J. W., Szundi, I., Briggs, W. R., and Bogomolni, R. a. (2001) The Photocycle of a Flavin-binding Domain of the Blue Light Photoreceptor Phototropin. *J. Biol. Chem. 276*, 36493–36500.

(60) Liu, Y., and Bell-Pedersen, D. (2006) Circadian rhythms in Neurospora crassa and other filamentous fungi. *Eukaryot. Cell 5*, 1184–1193.

(61) Gaidenko, T. a., Kim, T. J., Weigel, A. L., Brody, M. S., and Price, C. W. (2006) The blue-light receptor YtvA acts in the environmental stress signaling pathway of Bacillus subtilis. *J. Bacteriol. 188*, 6387–6395.

(62) Nelson, D. C., Lasswell, J., Rogg, L. E., Cohen, M. a, and Bartel, B. (2000) FKF1, a clock-controlled gene that regulates the transition to flowering in Arabidopsis. *Cell 101*, 331–340.

(63) Nash, A. I., Mcnulty, R., Elizabeth, M., Swartz, T. E., Bogomolni, R. A., and Luecke, H. (2012) Structural basis of photosensitivity in a bacterial light-oxygen-voltage/helix-turn-helix (LOV-HTH) DNA-binding protein. *Proc. Natl. Acad. Sci. 109*, 5904–5904.

(64) Habuchi, S., Ando, R., Dedecker, P., Verheijen, W., Mizuno, H., Miyawaki, A., and Hofkens, J. (2005) Reversible single-molecule photoswitching in the GFP-like fluorescent protein Dronpa. *Proc. Natl. Acad. Sci. U. S. A. 102*, 9511–9516.

(65) Mizuno, H., Dedecker, P., Ando, R., Fukano, T., Hofkens, J., and Miyawaki, A. (2010) Higher resolution in localization microscopy by slower switching of a photochromic protein. *Photochem. Photobiol. Sci. 9*, 239–248.

(66) Zhou, X. X., Chung, H. K., Lam, a. J., and Lin, M. Z. (2012) Optical Control of Protein Activity by Fluorescent Protein Domains. *Science (80-.). 338*, 810–814.

(67) Jenkins, G. I. (2014) The UV-B photoreceptor UVR8: from structure to physiology. *Plant Cell 26*, 21–37.

(68) Jenkins, G. I. (2009) Signal transduction in responses to UV-B radiation. *Annu. Rev. Plant Biol. 60*, 407–431.

(69) Heijde, M., and Ulm, R. (2013) Reversion of the Arabidopsis UV-B photoreceptor UVR8 to the homodimeric ground state. *Proc. Natl. Acad. Sci. U. S. A. 110*, 1113–8.

(70) Chen, D., Gibson, E. S., and Kennedy, M. J. (2013) A light-triggered protein secretion system. *J. Cell Biol. 201*, 631–640.

(71) Friedl, P., and Weigelin, B. (2008) Interstitial leukocyte migration and immune function. *Nat. Immunol. 9*, 960–9.

(72) Germain, R. N. (2002) T-cell development and the CD4-CD8 lineage decision. *Nat. Rev. Immunol. 2*, 309–322.

(73) Cyster, J. G. (2003) Lymphoid organ development and cell migration. *Immunol. Rev. 195*, 5–14.

(74) Moser, B., and Willimann, K. (2004) Chemokines: role in inflammation and immune surveillance. *Ann. Rheum. Dis. 63 Suppl 2*, ii84–ii89.

(75) Thelen, M., and Stein, J. V. (2008) How chemokines invite leukocytes to dance *9*, 953–959.

(76) Rossi, D., and Zlotnik, a. (2000) The biology of chemokines and their receptors. *Annu. Rev. Immunol. 18*, 217–42.

(77) Viola, A., and Luster, A. D. (2008) Chemokines and their receptors: drug targets in immunity and inflammation. *Annu. Rev. Pharmacol. Toxicol. 48*, 171–97.

(78) Ward, S. G., and Marelli-Berg, F. M. (2009) Mechanisms of chemokine and antigen-dependent T-lymphocyte navigation. *Biochem. J. 418*, 13–27.

(79) Teicher, B. a., and Fricker, S. P. (2010) CXCL12 (SDF-1)/CXCR4 pathway in cancer. *Clin. Cancer Res. 16*, 2927–2931.

(80) Real, E., Faure, S., Donnadieu, E., and Delon, J. (2007) Cutting edge: Atypical PKCs regulate T lymphocyte polarity and scanning behavior. *J. Immunol. 179*, 5649–5652.

(81) Walker, J. W., Gilbert, S. H., Drummond, R. M., Yamada, M., Sreekumar, R., Carraway, R. E., Ikebe, M., and Fay, F. S. (1998) Signaling pathways underlying eosinophil cell motility revealed by using caged peptides. *Proc. Natl. Acad. Sci. U. S. A. 95*, 1568–1573.

(82) Goguen, B. N., Hoffman, B. D., Sellers, J. R., Schwartz, M. a., and Imperiali, B. (2011) Light-triggered myosin activation for probing dynamic cellular processes. *Angew. Chemie - Int. Ed. 50*, 5667–5670.

(83) Sun, X., Cheng, G., Hao, M., Zheng, J., Zhou, X., Zhang, J., Taichman, R. S., Pienta, K. J., and Wang, J. (2010) CXCL12 / CXCR4 / CXCR7 chemokine axis and cancer progression. *Cancer Metastasis Rev. 29*, 709–22.

(84) Crump, M. P., Gong, J. H., Loetscher, P., Rajarathnam, K., Amara, A., Arenzana-Seisdedos, F., Virelizier, J. L., Baggiolini, M., Sykes, B. D., and Clark-Lewis, I. (1997) Solution structure and basis for functional activity of stromal cell-derived factor-1; dissociation of CXCR4 activation from binding and inhibition of HIV-1. *EMBO J. 16*, 6996–7007.

(85) Takenawa, T., and Miki, H. (2001) WASP and WAVE family proteins: key molecules for rapid rearrangement of cortical actin filaments and cell movement. *J. Cell Sci. 114*, 1801–1809.

(86) Chemotaxis, L., Reif, K., Okkenhaug, K., Sasaki, T., Penninger, J. M., Vanhaesebroeck, B., and Cyster, J. G. (2004) Differential Roles for Phosphoinositide 3-kinases, p110 gamma and p110 delta, in Lymphocytes Chemotaxis and Homing. *J. Immunol.* 0–4.

(87) Hirsch, E., Lembo, G., Montrucchio, G., Rommel, C., Costa, C., and Barberis, L. (2006) Signaling through PI3Kγ : a common platform for leukocyte , platelet and cardiovascular stress sensing 29–35.

(88) Brock, C., Schaefer, M., Reusch, H. P., Czupalla, C., Michalke, M., Spicher, K., Schultz, G., and Nürnberg, B. (2003) Roles of G beta gamma in membrane recruitment and activation of p110 gamma/p101 phosphoinositide 3-kinase gamma. *J. Cell Biol. 160*, 89–99.

(89) Kurig, B., Shymanets, A., Bohnacker, T., Prajwal, Brock, C., Ahmadian, M. R., Schaefer, M., Gohla, A., Harteneck, C., Wymann, M. P., Jeanclos, E., and Nürnberg, B. (2009) Ras is an indispensable coregulator of the class IB

phosphoinositide 3-kinase p87/p110gamma. *Proc. Natl. Acad. Sci. U. S. A. 106*, 20312–20317.

(90) Roose, J. P., Mollenauer, M., Gupta, V. a, Stone, J., and Weiss, A. (2005) A Diacylglycerol-Protein Kinase C-RasGRP1 Pathway Directs Ras Activation upon Antigen Receptor Stimulation of T Cells A Diacylglycerol-Protein Kinase C-RasGRP1 Pathway Directs Ras Activation upon Antigen Receptor Stimulation of T Cells. *Society 25*, 4426–4441.

(91) Kremer, K. N., Kumar, A., and Hedin, K. E. (2012) Gai2 and ZAP-70 mediate RasGRP1 membrane localization and activation of SDF-1 induced T cell functions1. *J. Immunol. 187*, 3177–3185.

(92) Yoo, S. K., Deng, Q., Cavnar, P. J., Wu, Y. I., Hahn, K. M., and Huttenlocher, A. (2010) Differential Regulation of Protrusion and Polarity by PI(3)K during Neutrophil Motility in Live Zebrafish. *Dev. Cell 18*, 226–236.

(93) Arimura, N., and Kaibuchi, K. (2007) Neuronal polarity: from extracellular signals to intracellular mechanisms. *Nat Rev Neurosci 8*, 194–205.

(94) Lowery, L. A., and Van Vactor, D. (2009) The trip of the tip: understanding the growth cone machinery. *Nat. Rev. Mol. Cell Biol. 10*, 332–343.

(95) Chappell, J. C., Wiley, D. M., and Bautch, V. L. (2011) Regulation of blood vessel sprouting. *Semin. Cell Dev. Biol. 22*, 1005–1011.

(96) Dustin, M. L. (2008) T-cell activation through immunological synapses and kinapses. *Immunol. Rev. 221*, 77–89.

(97) Huse, M., Quann, E. J., and Davis, M. M. (2008) Shouts, whispers and the kiss of death: directional secretion in T cells. *Nat. Immunol. 9*, 1105–1111.

(98) Szekanecz, Z., Kim, J., and Koch, A. E. (2003) Chemokines and chemokine receptors in rheumatoid arthritis. *Semin. Immunol. 15*, 15–21.

(99) Kalluri, R., and Weinberg, R. a. (2009) The basics of epithelial-mesenchymal transition. *J. Clin. Invest. 119*, 1420–1428.

(100) Hanahan, D., and Weinberg, R. a. (2011) Hallmarks of cancer: The next generation. *Cell 144*, 646–674.

(101) Witthuhn, B. A., Quelle, F. W., Silvennoinen, O., Yi, T., Tang, B., Miura, O., and Ihle, J. N. (1993) JAK2 associates with the erythropoietin receptor and is tyrosine phosphorylated and activated following stimulation with erythropoietin. *Cell 74*, 227–236.

(102) Wojchowski, D. M., Gregory, R. C., Miller, C. P., Pandit, a K., and Pircher, T. J. (1999) Signal transduction in the erythropoietin receptor system. *Exp. Cell Res. 253*, 143–56.

(103) Ohashi, H., Maruyama, K., Liu, Y. C., and Yoshimura, a. (1994) Ligand-induced activation of chimeric receptors between the erythropoietin

receptor and receptor tyrosine kinases. *Proc. Natl. Acad. Sci. U. S. A. 91*, 158–62.

(104) Luo, K., and Lodish, H. F. (1996) Signaling by chimeric erythropoietin-TGF-beta receptors: homodimerization of the cytoplasmic domain of the type I TGF-beta receptor and heterodimerization with the type II receptor are both required for intracellular signal transduction. *EMBO J. 15*, 4485–96.

(105) Johnson, D. L., Farrell, F. X., Barbone, F. P., McMahon, F. J., Tullai, J., Hoey, K., Livnah, O., Wrighton, N. C., Middleton, S. a, Loughney, D. a, Stura, E. a, Dower, W. J., Mulcahy, L. S., Wilson, I. a, and Jolliffe, L. K. (1998) Identification of a 13 amino acid peptide mimetic of erythropoietin and description of amino acids critical for the mimetic activity of EMP1. *Biochemistry 37*, 3699–710.

(106) Wrighton, N. C., Balasubramanian, P., Barbone, F. P., Kashyap, A. K., Farrell, F. X., Jolliffe, L. K., Barrett, R. W., and Dower, W. J. (1997) Increased potency of an erythropoietin peptide mimetic through covalent dimerization. *Nat. Biotechnol. 15*, 1261–1265.

(107) Chrétien, S., Varlet, P., Verdier, F., Gobert, S., Cartron, J. P., Gisselbrecht, S., Mayeux, P., and Lacombe, C. (1996) Erythropoietin-induced erythroid differentiation of the human erythroleukemia cell line TF-1 correlates with impaired STAT5 activation. *EMBO J. 15*, 4174–4181.

(108) Herbst, R. S. (2004) Review of epidermal growth factor receptor biology. *Int. J. Radiat. Oncol. Biol. Phys. 59*, 21–26.

(109) Huang, E. J., and Reichardt, L. F. (2003) Trk receptors: roles in neuronal signal transduction. *Annu. Rev. Biochem. 72*, 609–642.

(110) Gallo, G., Lefcort, F. B., and Letourneau, P. C. (1997) The trkA receptor mediates growth cone turning toward a localized source of nerve growth factor. *J. Neurosci. 17*, 5445–5454.

(111) Das, K. P., Freudenrich, T. M., and Mundy, W. R. (2004) Assessment of PC12 cell differentiation and neurite growth: A comparison of morphological and neurochemical measures. *Neurotoxicol. Teratol. 26*, 397–406.

(112) Miller, S. I., Ernst, R. K., and Bader, M. W. (2005) LPS, TLR4 and infectious disease diversity. *Nat. Rev. Microbiol. 3*, 36–46.

(113) Zhong, H., May, M. J., Jimi, E., and Ghosh, S. (2002) The phosphorylation status of nuclear NF-κB determines its association with CBP/p300 or HDAC-1. *Mol. Cell 9*, 625–636.

(114) Kla, P., Bochet, C. G., Givens, R., Rubina, M., Popik, V., Kostikov, A., and Wirz, J. (2012) Photoremovable Protecting Groups in Chemistry and Biology : Reaction Mechanisms and Efficacy. *Chem. Rev. 113*, 119–191.

(115) Dai, Q., and Pruett, S. B. (2006) Ethanol suppresses LPS-induced toll-like receptor 4 clustering, reorganization of the actin cytoskeleton, and associated TNF-alpha production. *Alcohol. Clin. Exp. Res. 30*, 1436–1444.

(116) Kobayashi, M., Saitoh, S., Tanimura, N., Takahashi, K., Kawasaki, K., Nishijima, M., Fujimoto, Y., Fukase, K., Akashi-Takamura, S., and Miyake, K. (2006) Regulatory roles for MD-2 and TLR4 in ligand-induced receptor clustering. *J. Immunol. 176*, 6211–6218.

(117) Miller, J. C., Silverman, S. K., England, P. M., Dougherty, D. A., and Lester, H. A. (1998) Flash Decaging of Tyrosine Sidechains in an Ion Channel. *Neuron 20*, 619–624.

(118) Kagan, J. C., Su, T., Horng, T., Chow, A., Akira, S., and Medzhitov, R. (2008) TRAM couples endocytosis of Toll-like receptor 4 to the induction of interferon-beta. *Nat. Immunol. 9*, 361–368.

(119) Nairz, M., Sonnweber, T., Schroll, A., Theurl, I., and Weiss, G. (2012) The pleiotropic effects of erythropoietin in infection and inflammation. *Microbes Infect. 14*, 238–246.

(120) Muthukumaran, G., Kotenko, S., Donnelly, R., Ihle, J. N., and Pestka, S. (1997) Chimeric erythropoietin-interferon gamma receptors reveal differences in functional architecture of intracellular domains for signal transduction. *J. Biol. Chem. 272*, 4993–4999.

(121) Burger, J. a., and Kipps, T. J. (2006) CXCR4: A key receptor in the crosstalk between tumor cells and their microenvironment. *Blood 107*, 1761–1767.

(122) Chen, X., Tang, S., Zheng, J.-S., Zhao, R., Wang, Z.-P., Shao, W., Chang, H.-N., Cheng, J.-Y., Zhao, H., Liu, L., and Qi, H. (2015) Chemical

synthesis of a two-photon-activatable chemokine and photon-guided lymphocyte migration in vivo. *Nat. Commun. 6*, 7220.